

AD-A070 174

FLORIDA UNIV GAINESVILLE COASTAL AND OCEANOGRAPHIC --ETC F/6 20/4  
AN EXPERIMENTAL INVESTIGATION OF THE RICHARDSON NUMBER PROFILE --ETC(U)  
1975 G M POWELL N00014-68-A-0173-0016

UNCLASSIFIED

NL

| OF |  
AD  
A070174

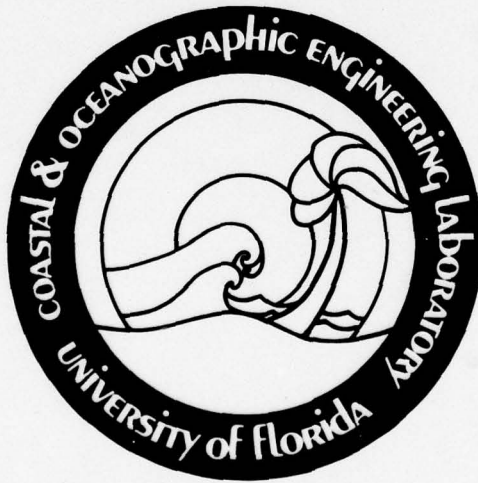


END  
DATE  
FILMED  
8-79  
DDC

LEVEL #

1

AD A070174



DDC  
RECEIVED  
JUN 15 1979  
RECEIVED

Handwritten mark resembling a stylized 'A' or 'S'.

C

DDC FILE COPY

COASTAL AND OCEANOGRAPHIC  
ENGINEERING LABORATORY

This document has been approved  
for public release and sale; its  
distribution is unlimited.

College of Engineering  
University of Florida  
Gainesville, Florida 32611

79 05 14 133

①

⑥ AN EXPERIMENTAL INVESTIGATION OF THE RICHARDSON  
NUMBER PROFILE IN A STRATIFIED SHEAR FLOW

⑨ Master's thesis,

by

⑩ Gregory M. Powell

DDC  
RECEIVED  
JUN 15 1979  
C

⑪ 1975

⑫

Contract ~~NO~~0014-68-A-0173-0016

⑬ 69e

A THESIS PRESENTED TO THE GRADUATE COUNCIL OF  
THE UNIVERSITY OF FLORIDA  
IN PARTIAL FULFILLMENT OF THE REQUIREMENTS FOR THE  
DEGREE OF MASTER OF ENGINEERING

UNIVERSITY OF FLORIDA

1975

This document has been approved  
for public release and sale; its  
distribution is unlimited.

408 006

5073

AN EXPERIMENTAL INVESTIGATION OF THE RICHARDSON  
NUMBER PROFILE IN A STRATIFIED SHEAR FLOW

by

Gregory M. Powell

A THESIS PRESENTED TO THE GRADUATE COUNCIL OF  
THE UNIVERSITY OF FLORIDA  
IN PARTIAL FULFILLMENT OF THE REQUIREMENTS FOR THE  
DEGREE OF MASTER OF ENGINEERING

UNIVERSITY OF FLORIDA

1975

to Carol

## ACKNOWLEDGEMENTS

Accession For	HTIS G. & I
	LCC TAB
	Unannounced
	Justification for the
By	<i>[Signature]</i>
Distribution/	
Availability Codes	
Dist	Avalland/or Special
	<i>A</i>

Many people have contributed their time and efforts toward the completion of this study. In particular the author would like to recognize his indebtedness to Dr. D. Max Sheppard for his continuous support and guidance. Without his help this thesis would not have reached this stage. The encouragement and contributions of Dr. Y. H. Wang are also greatly appreciated.

Thanks also go to John A. Videon and the Coastal Engineering Laboratory staff for their assistance with equipment for this experiment. For their determination and hard work the author wishes to thank Kathy Menezes, who patiently typed and re-typed this manuscript, and Ricardo A. Blue and Bruce Frendahl who drafted the figures.

A special thanks goes to fellow graduate students Ivan Chou and Tom Tomasello who shared in the fruits and frustrations of this project.

The author would like to take this opportunity to thank his parents for their unwavering support both spiritually and financially. He would also like to express his gratitude to all the teachers who contributed bits and pieces to his education.

Finally, the author wishes to thank his wife Carol for her help in editing the manuscript.

This work has been supported by the Fluid Mechanics Division of the Office of Naval Research under Contract N00014-68-A-0173-0016.

## TABLE OF CONTENTS

	Page
ACKNOWLEDGEMENTS .....	iii
LIST OF FIGURES .....	v
ABSTRACT .....	vii
CHAPTER	
I. INTRODUCTION .....	1
II. BACKGROUND THEORY .....	4
III. DESCRIPTION OF FLOW .....	10
IV. THE EXPERIMENT	
Facilities .....	13
Instrumentation .....	17
Procedure .....	30
V. RESULTS AND CONCLUSIONS .....	33
VI. FUTURE STUDIES .....	49
APPENDIX .....	50
BIBLIOGRAPHY .....	55
BIOGRAPHICAL SKETCH .....	57

## LIST OF FIGURES

Figure	Page
1. The Richardson Number Profile for Various Values of K, from Hazel (1972) .....	8
2. Definition Sketch .....	12
3. Schematic Drawing of the Overall Facility .....	14
4. Cross-sectional View of the Test Section .....	15
5. The Upstream End of Wave Tank .....	16
6. Black Box Schematic of the Instrumentation .....	18
7. Calibration Curve for Position Indication .....	20
8. Cross-section of Conductivity Probe .....	22
9. Conductivity Probe Voltage vs. Temperature .....	23
10. Schematic of Conductivity Probe Electronics .....	24
11. Calibration Curve for Conductivity Probe .....	25
12. Calibration Curves for Hot-film Anemometer .....	26
13. Calibration Curve for Thermistor .....	28
14. Schematic of Pre-Amp and Filter Circuits .....	29
15. Photographs of Interfacial Disturbance .....	36
16. Plot of Interface Position vs. Time .....	37
17. Initial Density Profile Before Shear Flow is Started ...	38
18. Velocity and Density Profiles, Run #5 .....	39
19. Richardson Number Profile, Run #5 .....	40
20. Velocity and Density Profiles, Run #12 .....	41
21. Richardson Number Profile, Run #12 .....	42



Figure	Page
22. Velocity and Density Profiles, Run #13 .....	43
23. Richardson Number Profile, Run #13 .....	44
24. Velocity and Density Profiles, Run #15 .....	45
25. Richardson Number Profile, Run #15 .....	46
26. Velocity and Density Profiles, Run #16 .....	47
27. Richardson Number Profile, Run #16 .....	48
28. Taylor Stability Model .....	51
29. Taylor and Goldstein Stability Model .....	52
30. Holmboe Stability Model .....	53
31. Hazel's Numerical Model .....	54

Abstract of Thesis Presented to the Graduate Council  
of the University of Florida in Partial Fulfillment  
of the Requirements for the Degree of Master of Engineering

AN EXPERIMENTAL INVESTIGATION OF THE RICHARDSON  
NUMBER PROFILE IN A STRATIFIED SHEAR FLOW

by

Gregory M. Powell

March, 1975

Chairman: Dr. D. M. Sheppard  
Major Department: Engineering Sciences

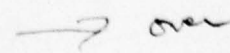
Stratified shear flows and the associated internal waves are often found in nature, both in the ocean and the atmosphere. The stability of this type of flow is governed by the Taylor-Goldstein equation

$$\phi'' - [(u-c)^{-1} u'' + (u-c)^{-2} (u')^2 R_i + k^2] \phi = 0$$

where the primes denote derivatives with respect to  $z$ ,  $\phi$  is the  $z$  dependence of the perturbation,  $u$  the primary flow velocity in the  $x$ -direction,  $c$  the complex phase speed of the disturbance, and  $k$  the disturbance wave number. The equation also contains, as a stability parameter, the local Richardson number

$$R_i(z) = \frac{-g\rho'(z)}{\rho(z)(u'(z))^2},$$

where  $\rho$  is the fluid density and  $g$  the acceleration of gravity.

The shear flow investigated in this thesis is one in which the density and velocity change rapidly across an interface between two miscible fluids. The Richardson number profile in the region of the interface is measured and the erosion of the interface is monitored periodically during the experiment. The interfacial erosion is then explained in terms of the gradient Richardson number profile. 

↘ A wave tank eighty feet long, four feet high, and two feet wide is used in this experiment. The fluid is stratified by varying the amount of salt dissolved in the water and the shear flow is created by pumping the upper layer in a closed circuit.

The results are presented as Richardson number profiles for various time durations and overall shear velocities. A plot of the interfacial position as a function of time is also included. ↗

*S. Max Sheppard*  
Chairman

## CHAPTER I INTRODUCTION

Stratified flows are often found in nature, both in the ocean and the atmosphere. With man's increased activity in the ocean, the atmosphere, lakes and estuaries, it becomes necessary to know under what conditions a stratified flow will become turbulent and what mechanisms are responsible for the instability.

The generation and subsequent breaking of internal waves is thought to be a major source of turbulence in stratified fluids. Theoretical studies indicate that a number of mechanisms may be responsible for the generation and growth of internal waves. The following are some of these mechanisms: unstable shear flows, interactions between internal waves of different frequencies and levels, interactions between surface and internal waves, flow over an undulating bottom, current oscillations (e.g. tidal fluctuations), and slowly moving pressure patterns above the free surface.

The vertical dispersion of salt, nutrients and pollutants in coastal and oceanic waters is an extremely important process in nature. Indeed, the entire ecosystem of most natural bodies of water is greatly influenced by this process. If the water is homogeneous, the mixing can be carried out by large-scale motions induced by winds, tides and evaporation-precipitation processes. When the water becomes stably stratified, however, as in the oceans and most lakes and estuaries, the large-scale motions are ineffective in the vertical mixing process and the small scale motions of turbulence become important.

In the atmosphere, the instability of a stratified shear flow can result in clear air turbulence (CAT), a threat to the comfort and safety of many airline passengers. A far more important aspects of CAT, however, is found in its meteorological implications. In the atmospheric boundary layer, the internal energy dissipation due to CAT may be on the order of one half of all the energy losses. This lack of knowledge about energy dissipation in the atmosphere is a major obstacle to the development of numerical models for weather predictions (Fleagle (1969) and Long (1972)).

The linearized stability equation for stratified shear flows is the so-called Taylor-Goldstein equation

$$\phi'' - [(u-c)^{-1} u'' + (u-c)^{-2} (u')^2 R_i + k^2] \phi = 0.$$

The primes denote derivatives with respect to  $z$ ,  $\phi$  is the  $z$  dependence of the perturbation,  $u$  the primary flow velocity in the  $x$ -direction,  $c$  the complex phase speed of the disturbance, and  $k$  the disturbance wave number. The equation contains, as a stability parameter, the local Richardson number

$$R_i = \frac{-g\rho'(z)}{\rho(z)(u'(z))^2}$$

where  $\rho$  is the mass density and  $g$  the acceleration of gravity. In order to solve the Taylor-Goldstein equation it is necessary to know the velocity and density profiles, and their derivatives, as functions of  $z$ . The Richardson number profile can then be calculated.

The experimental works to date dealing with interfacial instability and mixing appear to fall into two groups. The first group are those which generate the familiar Kelvin-Helmholtz instability at the interface. In these experiments the flow is accelerated rapidly to the point of instability, the instability grows rapidly and the collapse is catastrophic. The second group of experiments are those in which the interface tends to erode

with time. In this case the disturbances are manifest as small wavelets on the interface; the collapse of these disturbances does not radically change the character of the interface. The vertical mixing across the interface is, however, several times larger than that which can be explained by molecular diffusion.

The first objective of this research is to measure the actual velocity and density profiles at the interface between two miscible fluids in motion relative to one another; the Richardson number profiles will be calculated from this information. The second objective is to gain some insight into the mechanisms responsible for the mixing which takes place at the interface between the two fluids.

CHAPTER II  
BACKGROUND THEORY

As mentioned in the introduction, the linearized equation for the hydrodynamic stability of a stratified, incompressible, inviscid, shear flow is

$$\phi'' - [(u-c)^{-1} u'' + (u-c)^{-2} (u')^2 R_i + k^2] \phi = 0. \quad (1)$$

Note that the Boussinesq approximation (see Drazin and Howard, 1966) has been used in the development of this expression. This equation contains, as a stability parameter, the local or gradient Richardson number,

$$R_i(z) = \frac{-g\rho'}{\rho(u')^2} \quad (2)$$

Equation (1) written in terms of the Brunt-Väisälä frequency,  $N(z)$  is

$$\phi'' - [(u-c)^{-1} u'' + (u-c)^{-2} N^2(z) + k^2] \phi = 0, \quad (3)$$

where

$$N^2(z) \equiv \frac{-g\rho'(z)}{\rho(z)} \quad (4)$$

This equation has been called the Taylor-Goldstein equation after the two men who first derived it, Taylor (1931) and Goldstein (1931).

The solution to this equation requires a complete knowledge of both the density,  $\rho(z)$ , and the primary velocity  $u(z)$ , from which the Richardson number profile,  $R_i(z)$  can be obtained.

A sufficient condition for stability, as given by Miles (1961) and Howard (1961), (for the flow model given above) is that the local Richardson number be greater than 1/4 everywhere in the flow. This does not mean that the flow must become unstable if the local Richardson number falls

below  $1/4$ , nor does it mean that a turbulent flow must become laminar if the local Richardson number is everywhere greater than  $1/4$ . This theory only applies to the conditions under which an infinitesimal disturbance will decay. Transition from turbulent to laminar flow in a stratified shear flow has been observed (Woods, 1969) to occur when the Richardson number is of order one.

The analytical work done to date has been accomplished by assuming the shapes of the velocity and density profiles. Some of the assumed profiles are realistic; many of the others are not. The results of the analysis of some specific problems are presented in the Appendix. These results are helpful in establishing certain overall bounds on the stability but fail to yield specific information about physically obtainable flows. One important point brought into focus by the analytical work is that the character of the instability and the point of instability are both highly dependent upon the velocity and density profiles\*. The results of such analysis are normally presented as a neutral curve in the  $J$ - $\alpha$  plane. The parameter  $J$  has been defined two different ways in the literature. Some authors define  $J$  as an overall Richardson number,

$$J \equiv \frac{\Delta\rho gh}{\rho(\Delta u)^2},$$

where  $\Delta\rho$  is the difference in density between the upper and lower layers,  $\rho$  the average density,  $\Delta u$  the difference in velocity of the upper and lower layers,  $g$  the acceleration of gravity, and  $h$  the vertical length over which the velocity and/or the density change. Other authors define  $J$  as the

---

\*For a more detailed discussion of this point see Hazel (1972) and Howard and Moslowe (1972).



interfacial Richardson number.

$$J \equiv R_i(z_i)$$

In this definition  $z_i$  is located at the inflection point of the density profile. In either case  $J$  may or may not be the minimum Richardson number for the flow. It becomes evident after studying the different models that the solution to the stability problem depends upon the velocity and density profiles chosen, and upon the way in which  $J$  is defined.

The model which most accurately fits the velocity and density profiles obtainable in a real fluid is the numerical model developed by Hazel (1972). Hazel showed, using a hyperbolic tangent velocity and density profile (see Figure 31 of the appendix), that the characteristics of the instability change as the density transition layer becomes thinner compared to the velocity transition layer. Hazel defines his velocity profile by

$$u(\xi) = \tanh(\xi),$$

where  $\xi$  is a dimensionless vertical coordinate with its origin at the interface. The density profile is given by

$$\frac{1}{\sigma} \ln \left( \frac{\rho_0}{\rho} \right) = \frac{1}{K} \tanh(K\xi),$$

where  $\sigma$  is a typical density measure and  $\rho_0$  the density at  $\xi = 0$ . Note that the velocity and density profiles are symmetric about  $\xi = 0$ . The parameter  $K$  is used to vary the thickness of the density profile with respect to the velocity profile. As  $K$  grows larger, the thickness of the interface is reduced and the density profile approaches a step function. The changes in the stability characteristics coincide with changes in the shape of the Richardson number profile (see Figure 1).

Region I: ( $0 \leq K \leq \sqrt{2}$ ) In this case the Richardson number profile has a minimum value at  $\xi = 0$  and continuously increases with  $\xi$ ; so that  $R_i(\xi) \rightarrow \infty$  as  $\xi \rightarrow \infty$ .

Region II: ( $\sqrt{2} < K < 2$ ) In this case the Richardson number profile has a minimum value at some point above and below  $\xi = 0$ . The Richardson number is a local maximum at  $\xi = 0$  and  $R_i(\xi) \rightarrow \infty$ , as  $\xi \rightarrow \infty$ .

Region III: ( $K \geq 2$ ) In this case the Richardson number profile has an absolute maximum at  $\xi = 0$  and  $R_i(\xi) \rightarrow 0$ , as  $\xi \rightarrow \infty$ .

The experimental work in this area can generally be divided into two groups based on either the method used to generate the shear flow or the disturbance which results. If the shear flow is generated by rapidly accelerating the fluid from rest the resultant velocity and density transition layers are approximately the same thickness. This method has been used by Scotti and Corcos (1969) and also by Thorpe (1969). The velocity profile produced in this way is directly related to the density profile through the inertia terms in the Navier-Stokes equations. The instability which dominates in this case is of the Kelvin-Helmholtz type. The resultant Richardson number profile for a flow generated in this manner corresponds to Region I of Hazel's model, and the minimum Richardson number falls at the interface. The other method of creating a shear flow is to pump the upper and/or the lower fluid separate from one another. This procedure results in a velocity profile that is only slightly dependent upon the density profile and highly dependent upon the viscosity of the fluid. The Richardson number profile generated in this manner is generally of the type found in Regions II and III of Hazel's model, with the minimum Richardson number falling above and/or below the interface. The interfacial Richardson number may be a local maximum in this case. This method has been used by Wang (1972), Keulegan (1949), and Broward and Winant (1972); it is also the method used in this experiment. The disturbance produced

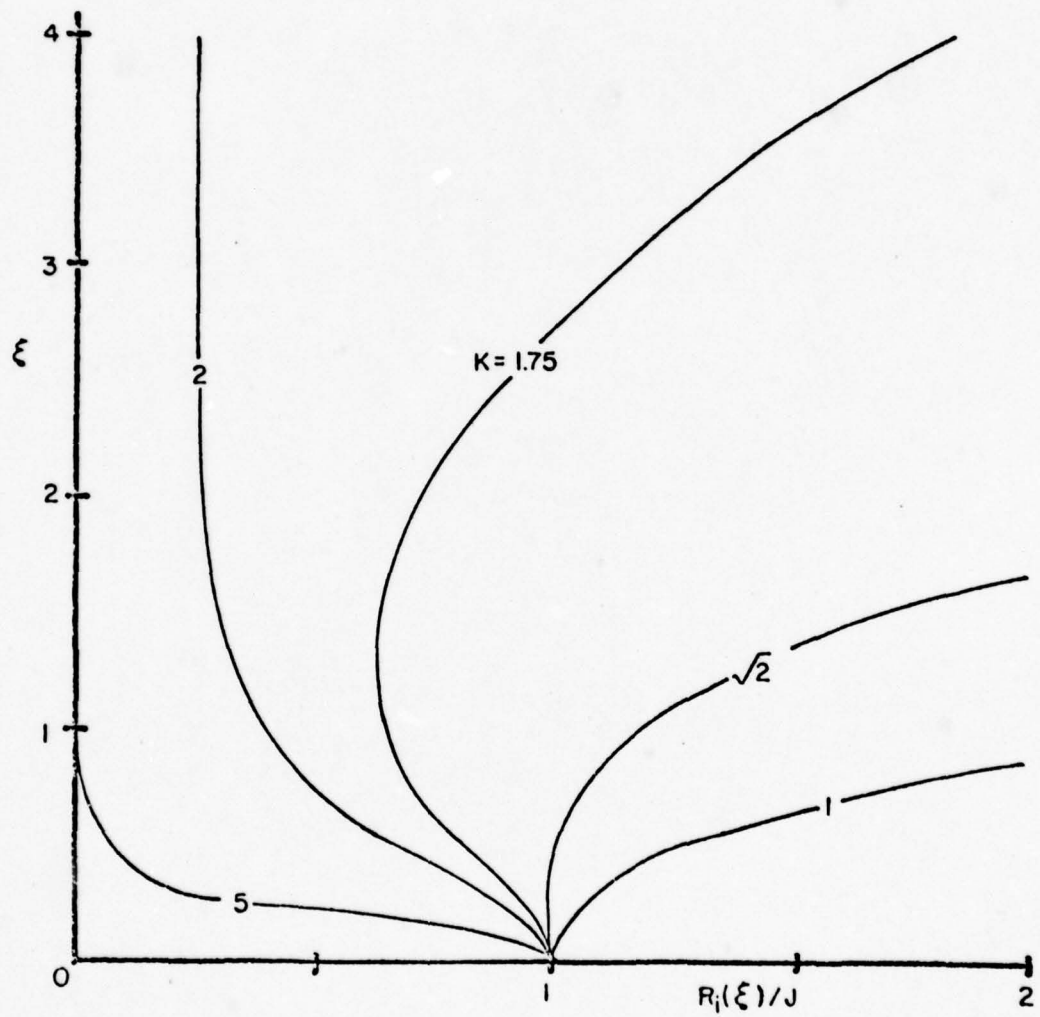


Figure 1. The Richardson Number Profile for Various Values of  $K$ , from Hazel (1972)

by this type flow does not exhibit the regularity and symmetry of the Kelvin-Helmholtz instability but manifests itself as wavelets on the interface.

The rate of "erosion" of the interface (i.e. the rate of drop of the interface) is known to increase as the shear flow is increased above some critical value (Keulegan, 1949). A possible mechanism responsible for this phenomena may be the existence of an unstable region just above the interface where infinitesimal disturbances are able to grow to some finite level. This unstable region may, however, be bounded from below and/or from above by regions where the Richardson number is very large. Any disturbances which try to propagate into these regions of large Richardson number would be quickly damped. One objective of this thesis is to investigate this possibility by experimentally determining Richardson number profiles in a two layer stratified shear flow.

### CHAPTER III DESCRIPTION OF FLOW

The flow studied for this experiment is characterized by two thick layers of nearly uniform density fluid, separated by a thin transition region in which the density changes rapidly (see Figure 2). In Figure 2 the thickness of the transition layer has been exaggerated with respect to the overall depth,  $D$ . In the actual flow the transition region is only about 4% of the total depth. The density stratification is produced by varying the amount of dissolved salt.

The upper layer, which initially contains almost no salt, is pumped in a closed circuit. The flow exits at the downstream end of the test section, is pumped through a 6 inch PVC pipe, and re-enters the test section at the upstream end. The velocity profile generated in this manner will be nearly uniform in the fresh water layer, will vary rapidly near the interface, and become zero a small distance into the salt layer. In general the velocity and density will vary in the vertical and horizontal directions and time. Since the horizontal variations in density and velocity are significant only near the entrance and exit, and since the measurements are taken near the middle of the tank, horizontal variations will not be considered. The flow will be considered two dimensional and the velocity and density profiles will be rapidly varying functions of the vertical coordinate (near the interface) and slowly varying functions of time.

Since the objective of this study is to investigate the mechanisms

responsible for the mixing which takes place at the interface, only the region surrounding the interface is of interest. This region is thin compared to the overall depth; and the wave lengths associated with the disturbances which form at the interface are short compared to the depth of flow, thus the free surface and bottom are assumed to have no effect on the interfacial mixing process.

Due to the small velocities, the flow in the lower layer is always laminar. The upper layer, however, can not be considered laminar since the Reynold number, based on the hydraulic radius, is about 6500. The turbulent intensity, as defined below, is very small.

$$\sqrt{(u')^2} / \bar{u} < 1\%$$

where  $\bar{u}$  is the mean time averaged velocity and  $u'$  is the velocity fluctuation about  $\bar{u}$ .

There are two coordinate systems referred to in this thesis (see Figure 2 ). The Z-coordinate is fixed with respect to the tank; Z is positive upward and Z=0 is at the bottom of the tank. The  $\xi$ -coordinate is free to move with the density interface;  $\xi=0$  is defined as the point where the density is equal to the average density of the upper and lower layers,

$$\rho(\xi=0) = \frac{\rho_U + \rho_L}{2} ,$$

where  $\rho_U$  is the density of the upper layer and  $\rho_L$  is the density of the lower layer. The relationship between the two coordinate systems is

$$Z = \xi + d_2(t)$$

where  $d_2(t)$ , the vertical distance between  $\xi=0$  and the bottom of the tank, is a slowly varying function of time. The total distance between the free surface and the bottom of the tank is given by D, which does not vary with time.

$$D = 48 \text{ inches}$$

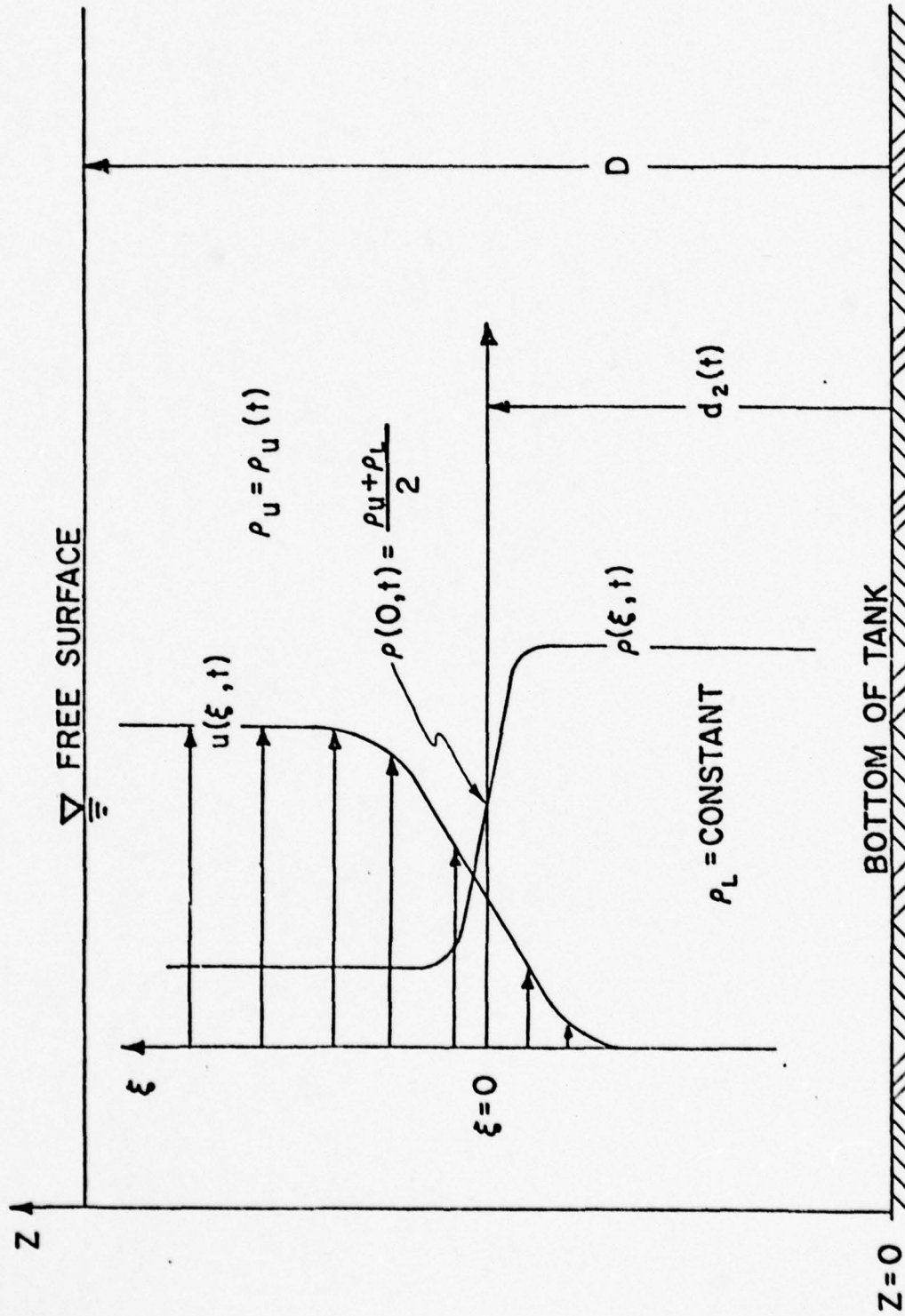


Figure 2. Definition Sketch

## CHAPTER IV THE EXPERIMENT

### Facilities

The internal wave tank located at the University of Florida Coastal and Oceanographic Engineering Lab was used in this experiment. The internal wave tank was designed as a multipurpose facility; and therefore, has many operational features not required for this study. For the purpose of clarity, however, a description of the total facility will be given below. Figure 3, a schematic drawing of the overall facility, shows the location of the main components and the more important dimensions.

The test section of the tank is 80 feet long, 6 feet high and 2 feet wide in the lower portion and 3 feet wide in the upper wind tunnel section. Figure 4 shows a cross-sectional view of the test section. In this experiment, the bottom one-third of the test section is filled with salt water and the middle one-third with fresh water. The upper one-third of the tank is a wind tunnel used to generate wind waves and wind-induced currents. The sides of the test section are made of 1/2 inch thick glass panels; allowing visual observation of the flow from both sides. The wave tank is capable of mechanically generating surface waves and internal waves at the interface between the fresh and salt water.

Shear flows can be produced by pumping the upper layers in a closed circuit. In this experiment only the shear flow capability was required. The pumping system includes two centrifugal pumps connected in parallel. One pump is 60 hp and can produce flow rates up to approximately 1 ft/sec.



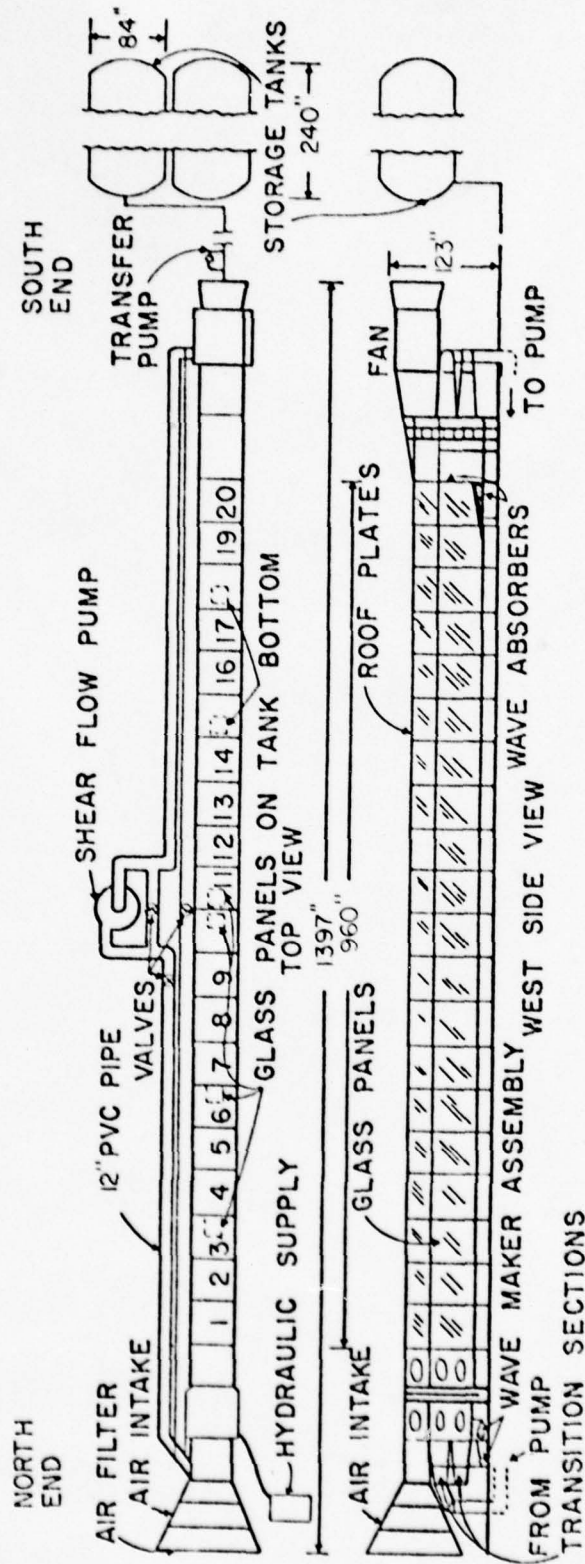


Figure 3. Schematic Drawing of the Overall Facility

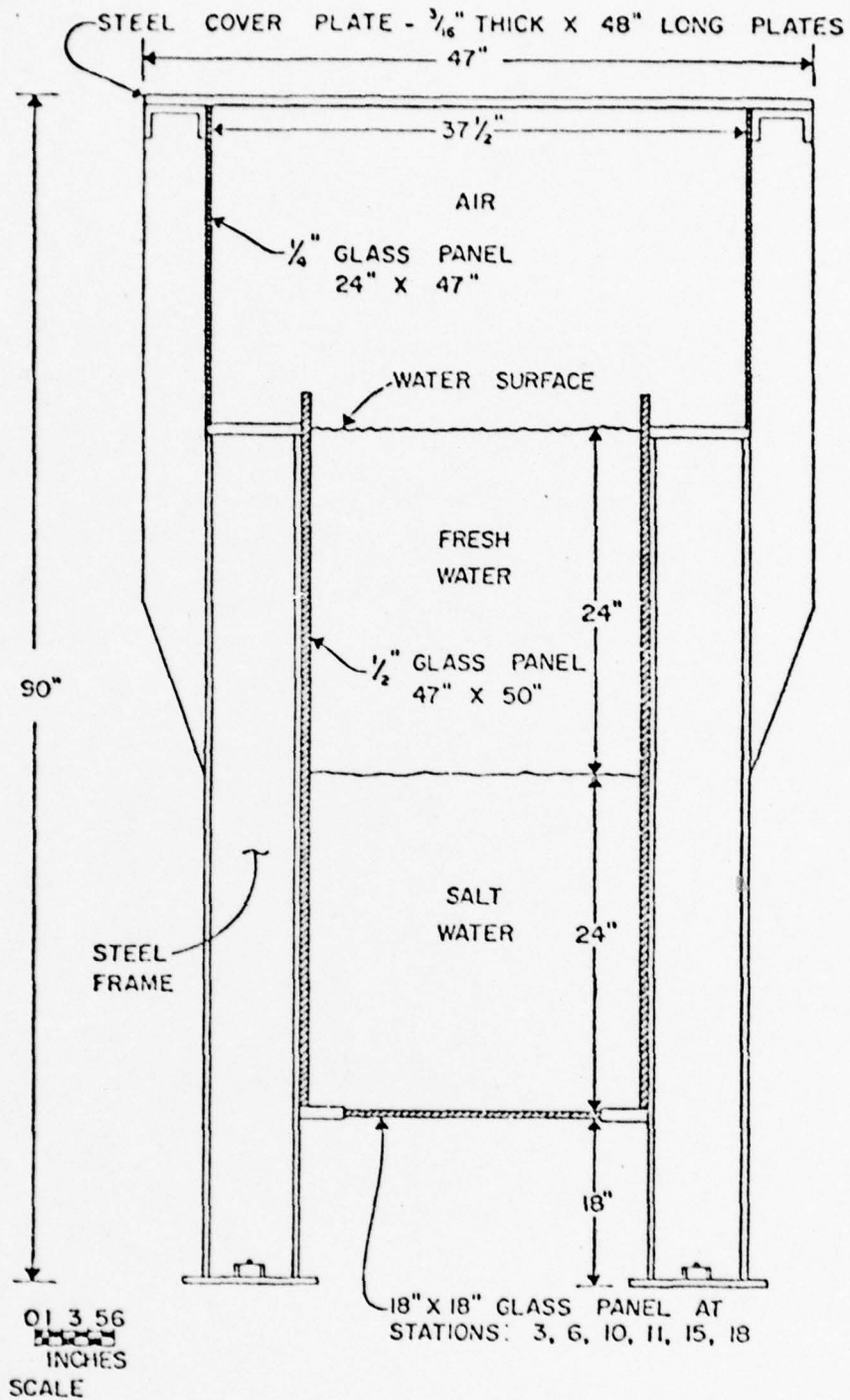


Figure 4. Cross-sectional View of the Test Section

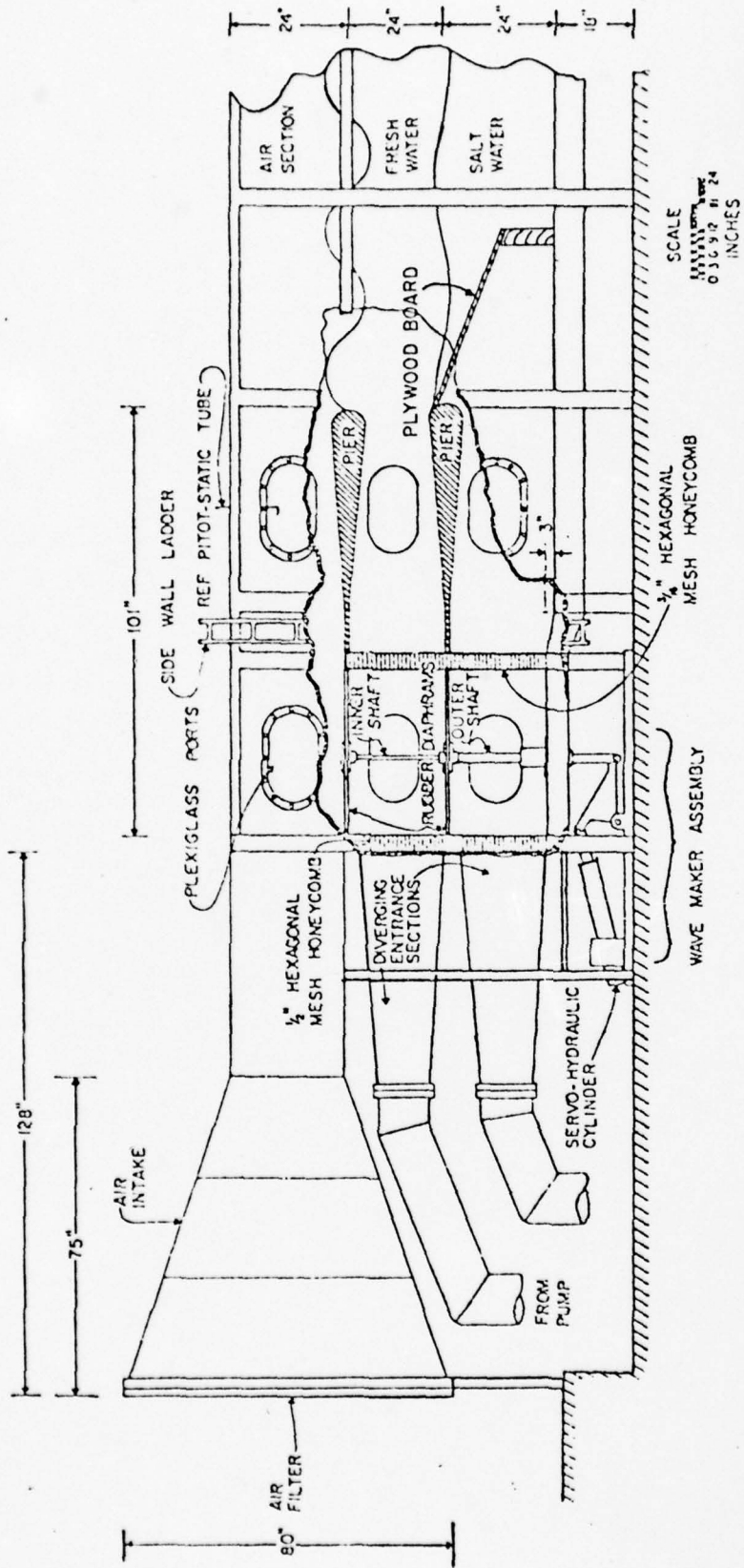


Figure 5. The Upstream End of Wave Tank

However, at low flow rates (less than 3 in/sec) this pump heats the water excessively and is hard to control. The other pump is only 5 hp and can produce flows up to approximately 3 in/sec. Therefore, for flows up to 3 in/sec the small pump is used to minimize thermal stratification in the tank.

Since the internal wave generator was not used during this experiment, the pier at the interface between the fresh and salt water was modified to allow the upper flow to smoothly meet the stagnant lower fluid, and to reduce disturbances caused by flow separation around the pier. To accomplish this, a 1/4 inch thick plywood board was attached to the top of the pier. The board was allowed to extend downward into the salt layer; entering the salt water at a small angle (see Figure 5). To reduce large scale disturbances to the flow, hexagonal mesh honeycomb flow straighteners are located upstream of the entrance to the test section.

#### Instrumentation

The objective of this experiment is to determine the Richardson number profile in a stratified shear flow as a function of the vertical coordinate. The determination of the Richardson number profiles requires, however, a knowledge of both the density and velocity profiles. The instrumentation for this experiment was designed to obtain both profiles simultaneously as a function of the vertical coordinate. A description of the instrumentation system and its components is given below.

Figure 6 is a black box schematic of the instrumentation set-up. For this experiment the internal wave gauges were not required. A vertical traverse mechanism is mounted on top of the wave tank. Attached to the end of the traverse is an instrument package that contains a wedge-type

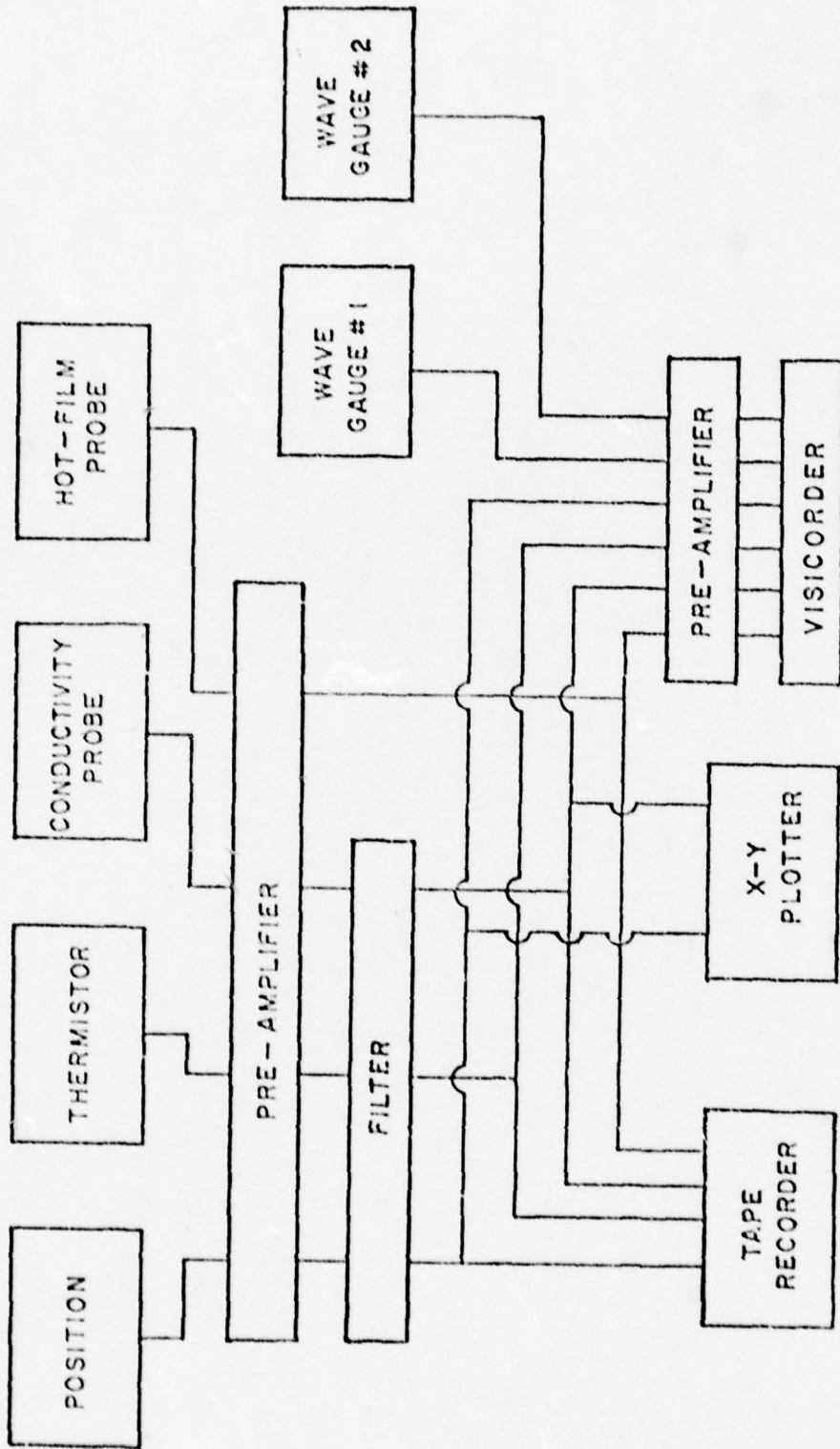


Figure 6. Black Box Schematic of the Instrumentation

hot-film probe, a glass bead thermistor, and a two-electrode conductivity probe. All three probes are mounted at the same level and are horizontally spaced about 1/2 inch apart. The horizontal spacing is enough that disturbances generated by one probe will not significantly affect the other probes. The hot-film probe is mounted slightly forward of the others in order to further reduce any effects the other probes may have on the velocity reading.

Since the region of interest is no more than 4 inches thick, the first, and most severe requirement imposed upon the instrumentation, was that the vertical resolution be on the order of 0.025 inch. This requirement made the development of specialized instrumentation necessary.

The Traverse Mechanism: This unit was designed and built specifically for the internal wave tank, and is driven by a 1/2 hp, variable speed, DC electric motor. The traverse can move only in the vertical direction, from a point near the free surface to a point 17 inches from the bottom; a total distance of 28 inches. The unit may be stopped and started manually or may be set to shuttle back and forth between any two points at any speed between zero and approximately 6 in/sec. As the traverse mechanism moves, it drives a ten-turn, 10K, potentiometer. The potentiometer is part of a DC circuit designed to give a linear output voltage proportional to the position of the traverse (see insert in Figure 7). The linearity of the potentiometer is 0.05%; therefore, the calibration curve is almost a straight line (see Figure 7). This circuit is very stable and the position can be determined within  $\pm 0.025$  inch.

The Conductivity Probe: The conductivity probe is a modified form of the probe designed by Sheppard and Doddington (submitted for publication in Review of Scientific Instrumentation). The modifications consisted of

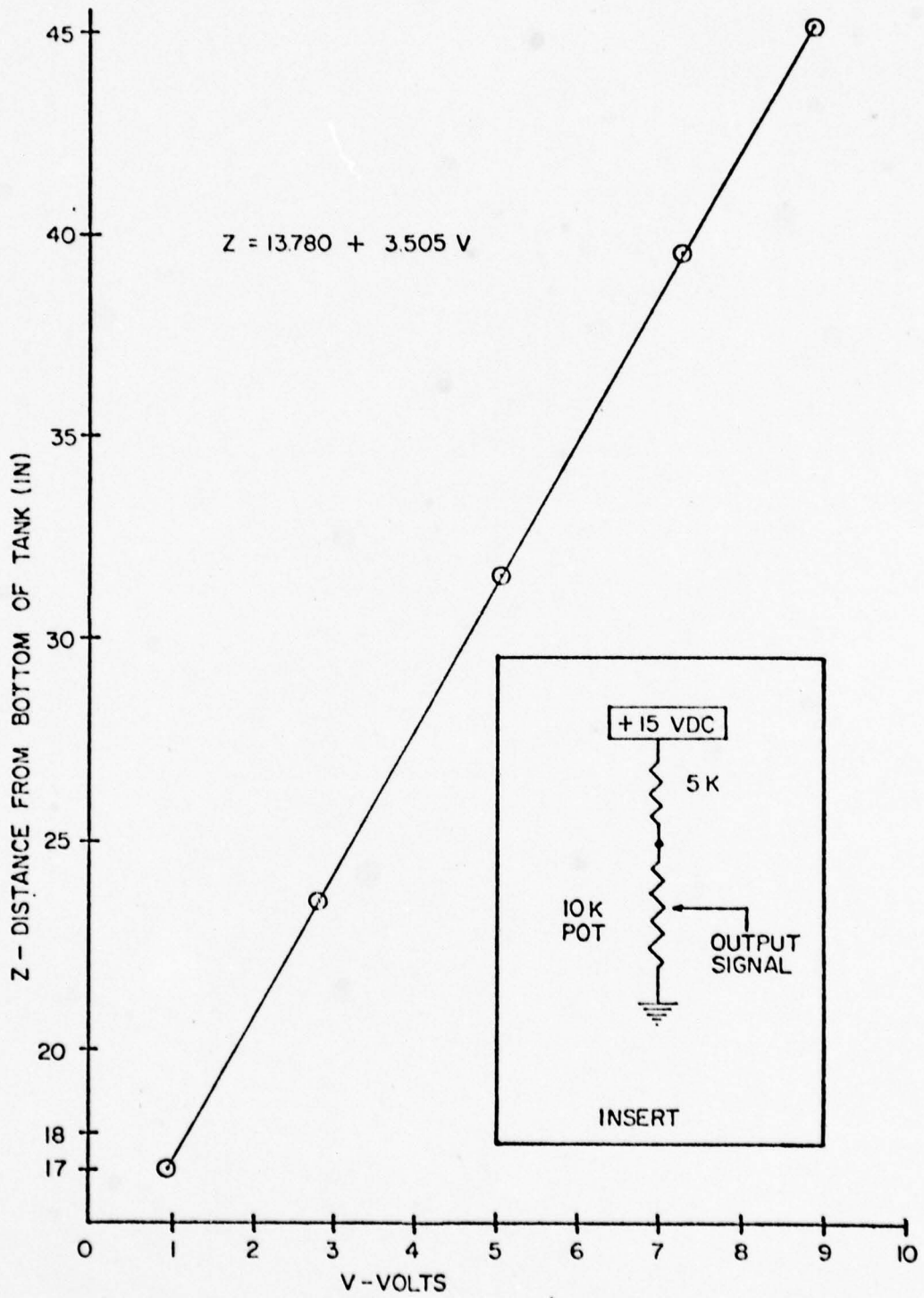


Figure 7. Calibration Curve for Position Indication

only slight changes in shape and size; the principles of operation, however, are identical. This probe has two important features not found in most conductivity probes. The first, is that it can measure the conductivity at any level with a vertical resolution of less than 0.025 inch. It does this by drawing the fluid in through a horizontal slit in the probe tip (see Figure 8). The process of selective withdrawal allows the probe to draw fluid from only one density level. The second important feature of this probe is that it employs two relatively large electrodes. This reduces the low frequency drift problems associated with small electrode conductivity probes. Tests, conducted to determine the effect of temperature changes on the probe output voltage, indicate only a slight temperature dependence (see Figure 9). Figure 10 is a schematic of the conductivity probe electronics. This probe has a limited life time, and aging does change the calibration curve; however, for time spans up to about one day the probe is very stable. For this experiment the probe was calibrated at the start of each test, which never lasted more than a few hours. The conductivity probe calibration curve for this experiment is shown in Figure 11.

The Velocity Probe: The velocity of the flow was measured with a constant temperature hot-film anemometer manufactured by Thermo-Systems, Inc. The system consists of a Model 1051 power supply and monitor unit, a Model 1050 bridge unit, a Model 1055 linearizer and a wedge-type hot-film sensor, Model 1233 NaCl. The hot-film probe was calibrated in fresh water as well as several solutions of salt water having specific gravities up to 1.0315. The calibration curves are shown in Figure 12. The effect of salinity on the anemometer reading is not insignificant; therefore, when the data were reduced the output voltage was corrected for salt concentration



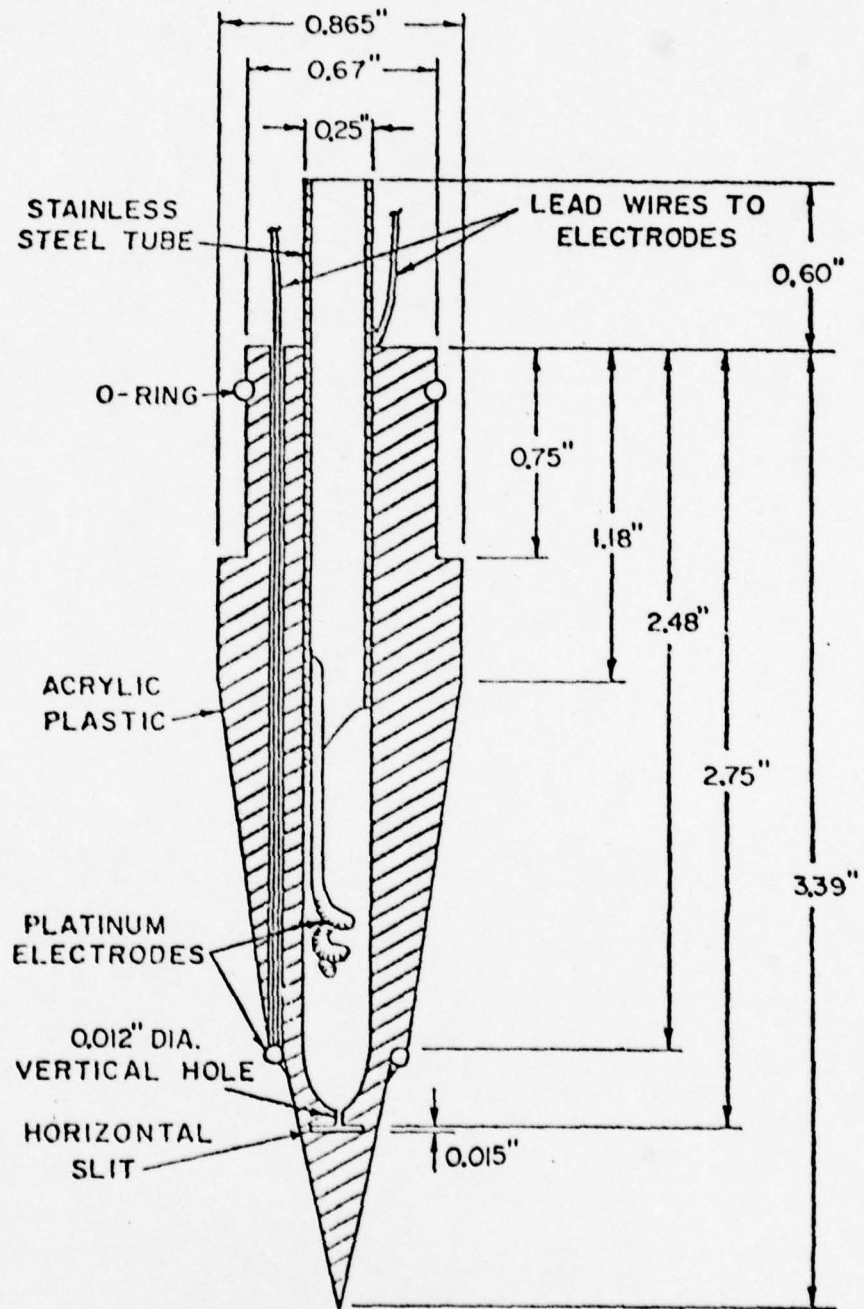


Figure 8. Cross-section of Conductivity Probe

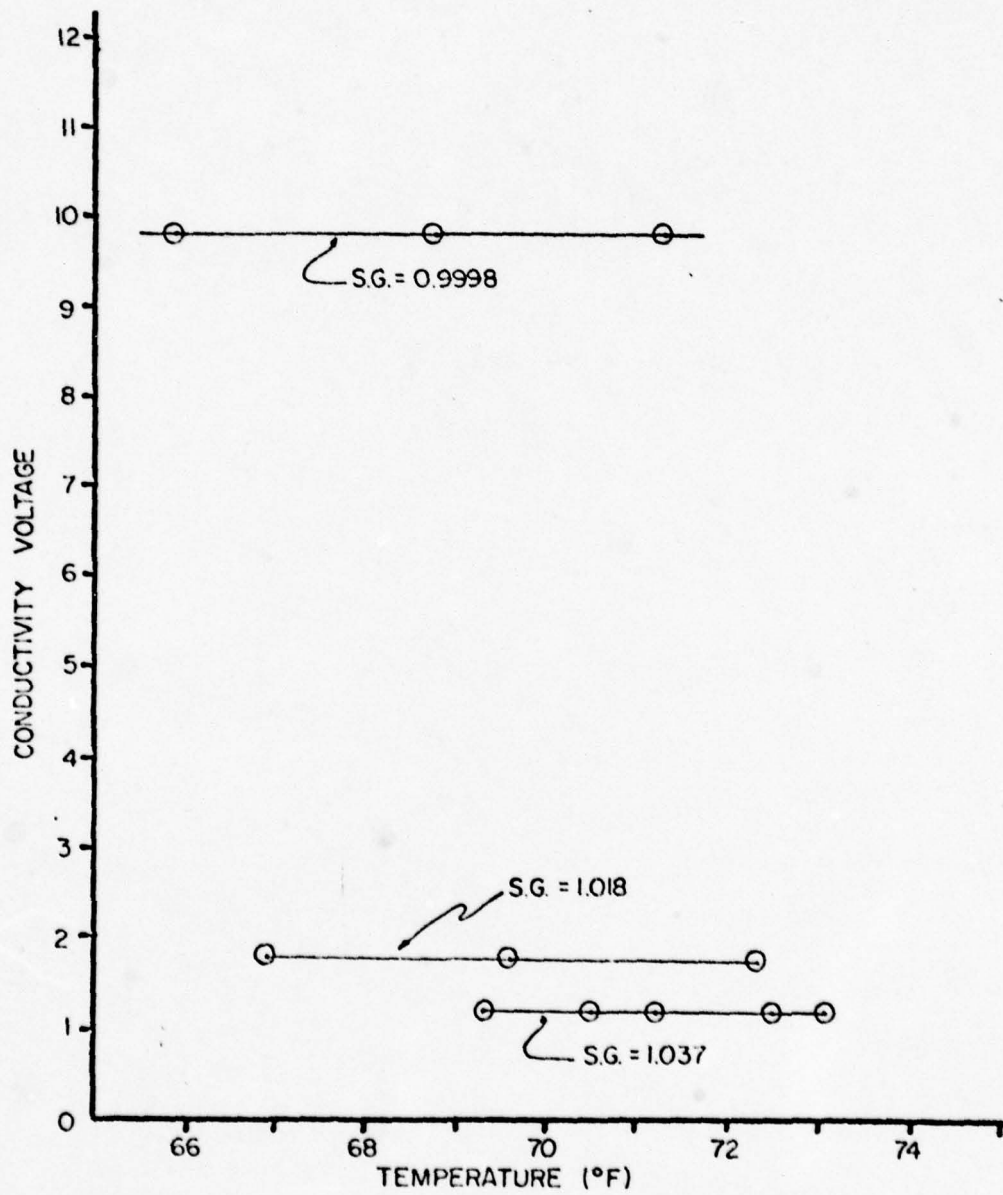


Figure 9. Conductivity Probe Voltage vs. Temperature

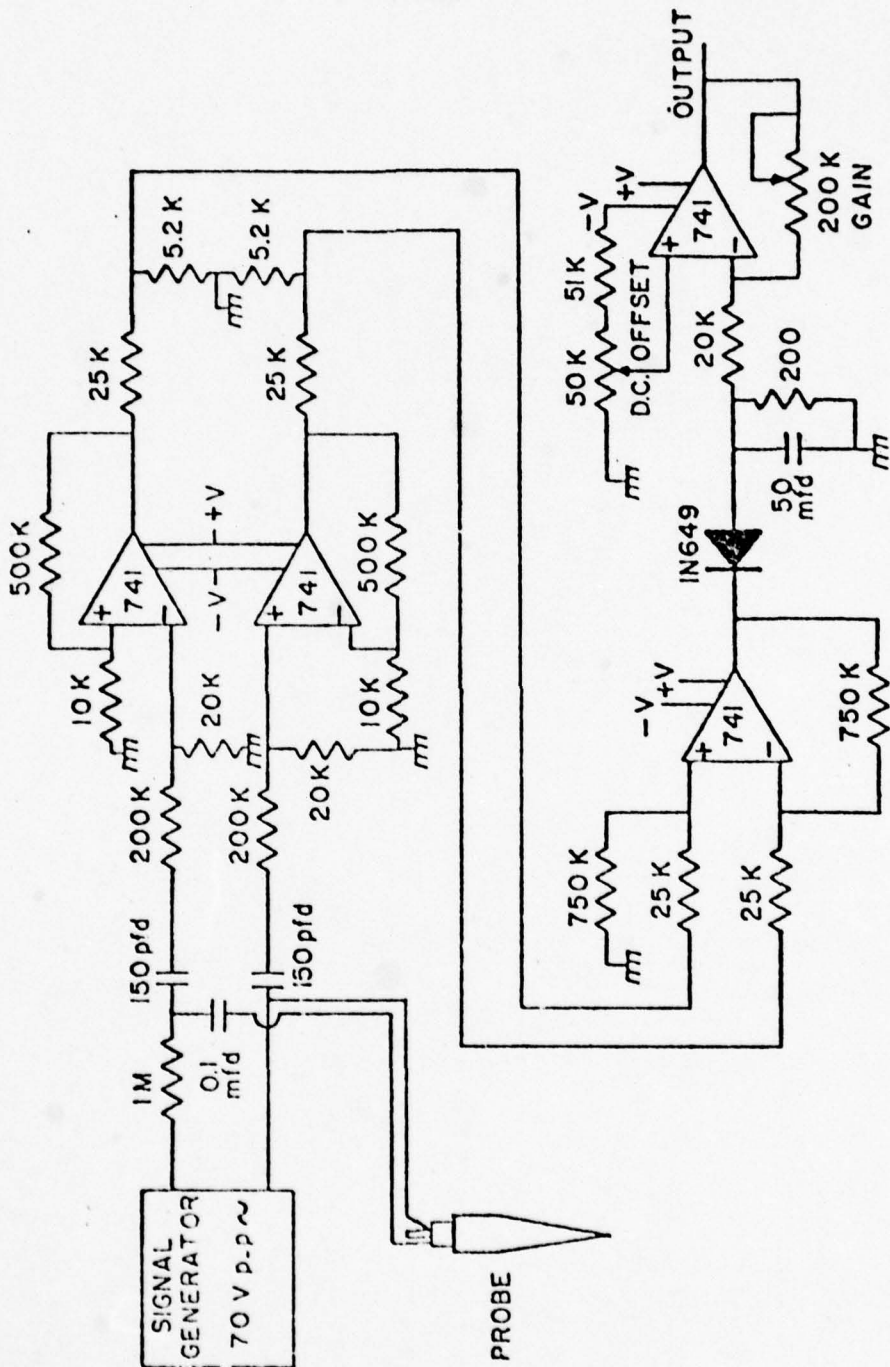


Figure 10. Schematic of Conductivity Probe Electronics

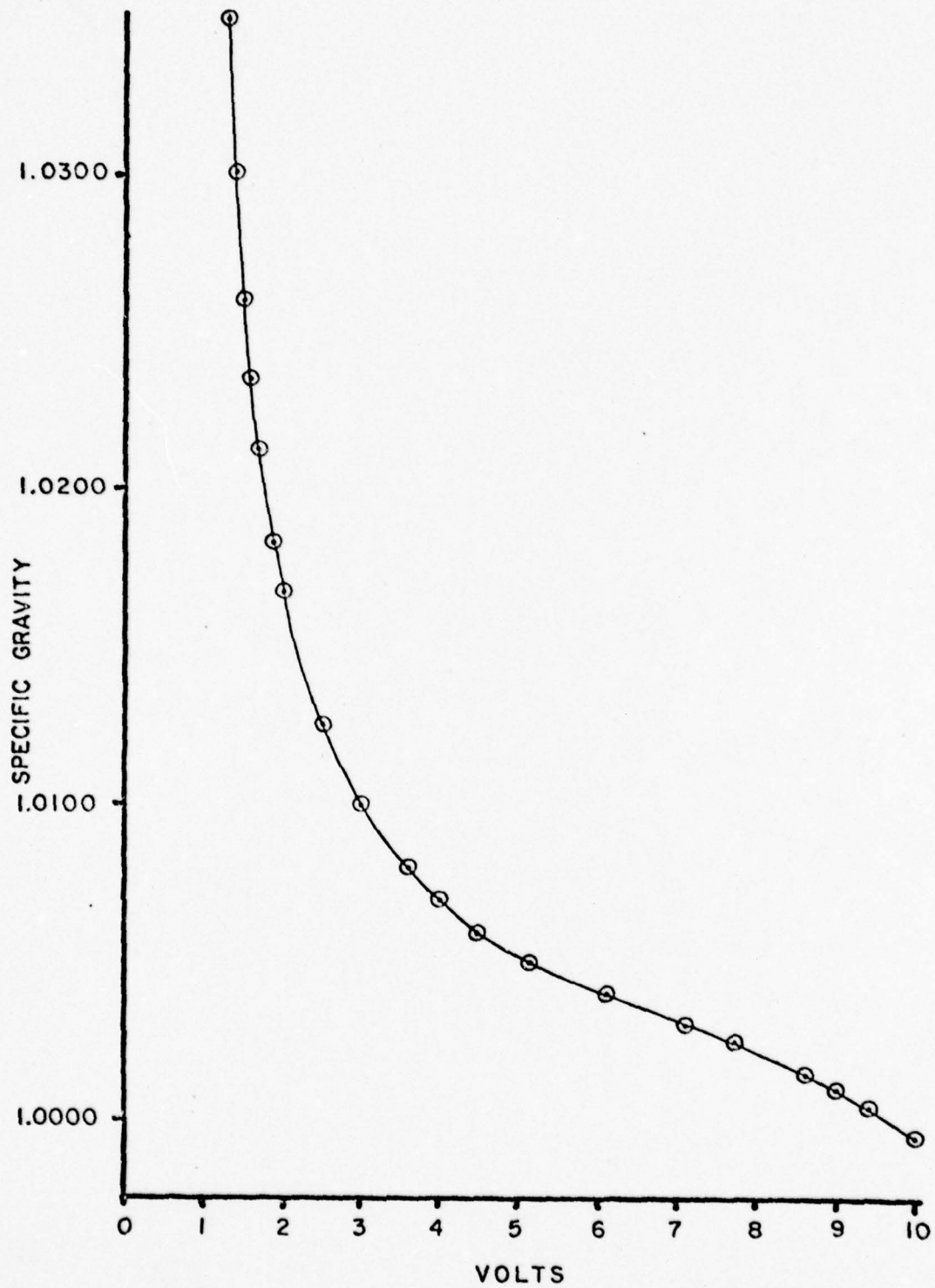


Figure 11. Calibration Curve for Conductivity Probe

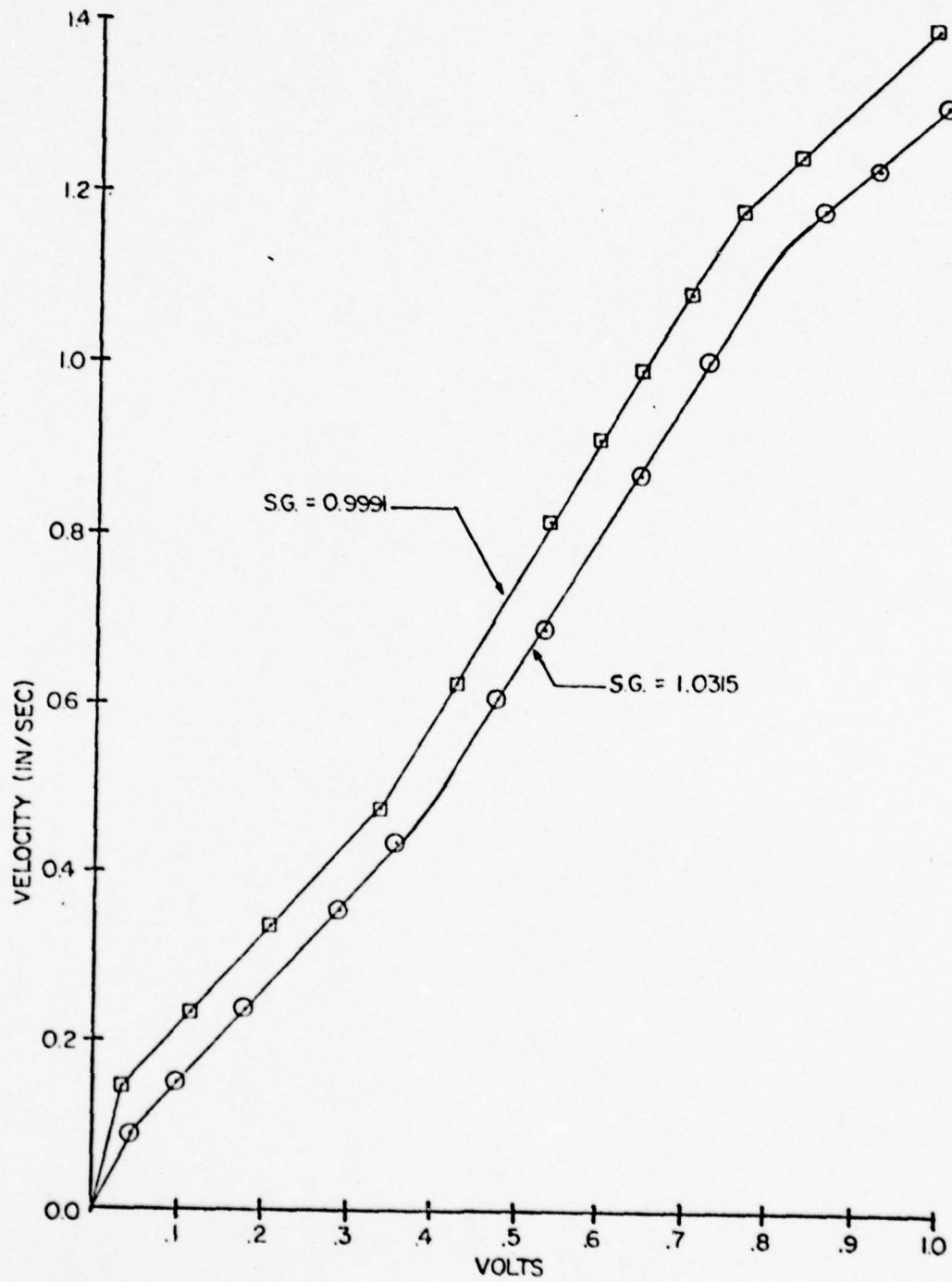


Figure 12. Calibration Curves for Hot-film Anemometer

effects. An overheat ratio of 1.05 was used in these tests. When larger overheat ratios were used, bubbles formed on the probe tip in the salt solutions.

The Temperature Probe: The temperature was measured using a glass bead thermistor manufactured by Keystone Carbon Company. It is an experimental model, Type 08127401, designed for use in salt water. The thermistor is placed in a low output impedance circuit, which gives an output voltage proportional to the temperature of the fluid. The thermistor was calibrated using a thermometer with 0.2°F divisions. The thermistor calibration curve, shown in Figure 13, is almost linear. The calibration curve was checked periodically and it was found that the curve shifted slightly over long periods of time; however, the slope and shape of the curve always remained constant.

The Tape Recorder: A four-channel, FM tape recorder, Model 3960A, manufactured by Hewlett Packard was used to record the output voltage from all four sources (position indicator, thermistor, hot-film, and conductivity probe) simultaneously.

The X-Y Plotter: An Omnigraphic 2000 Recorder, Type 6, manufactured by Houston Instrument was used during the tests to plot the conductivity vs. position. This gave a visual display of the probe position with respect to the interface, and also provided a check on the instrumentation drift during the tests.

The Pre-Amplifier and Low-Pass Filter: The four-channel pre-amp and low pass filter was placed in series with the four sensors. This unit is designed to filter out electrical noise, picked up from equipment located in the laboratory, and to match the sensor output voltage with the maximum allowable input voltage of the tape recorder. This unit has a high

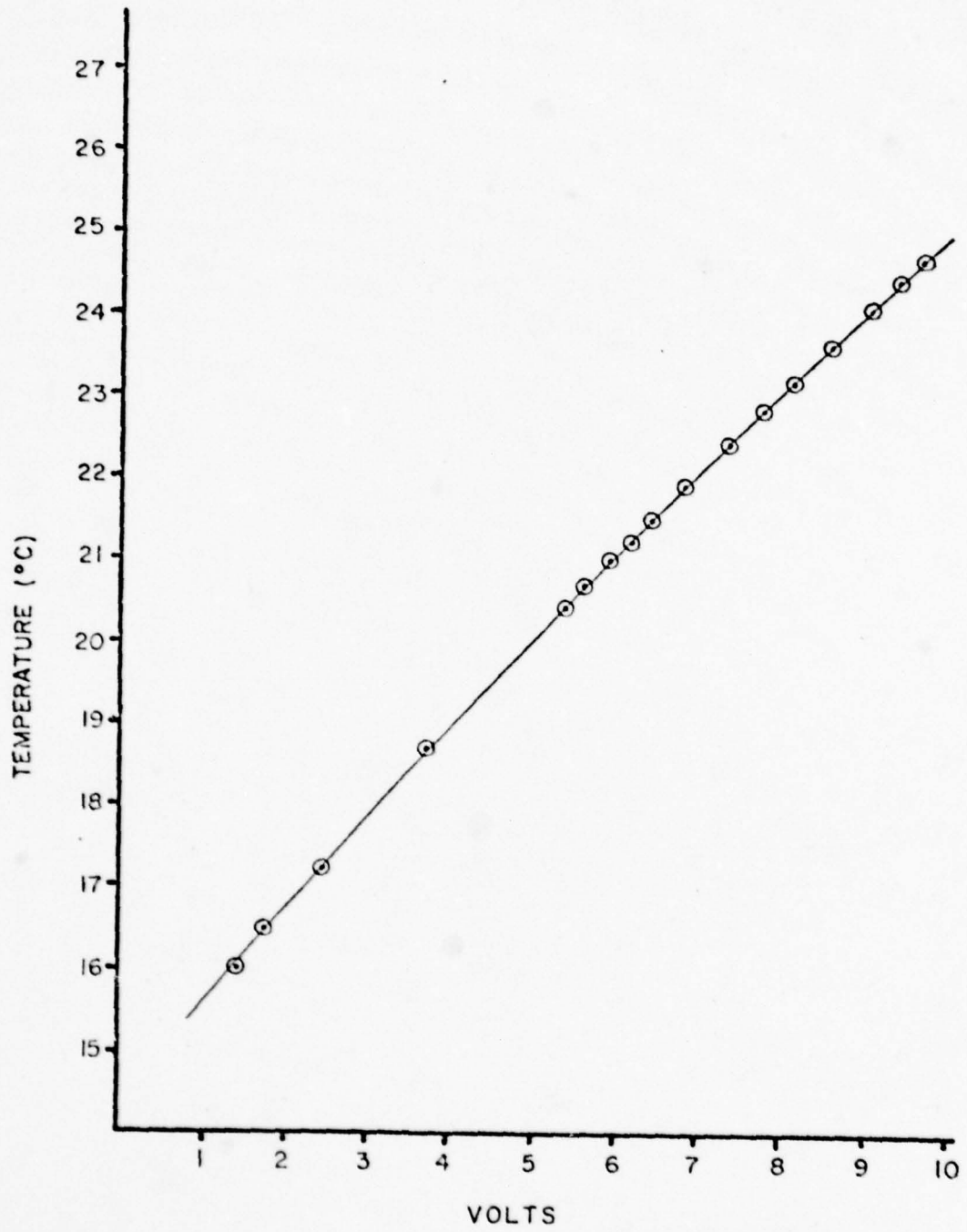
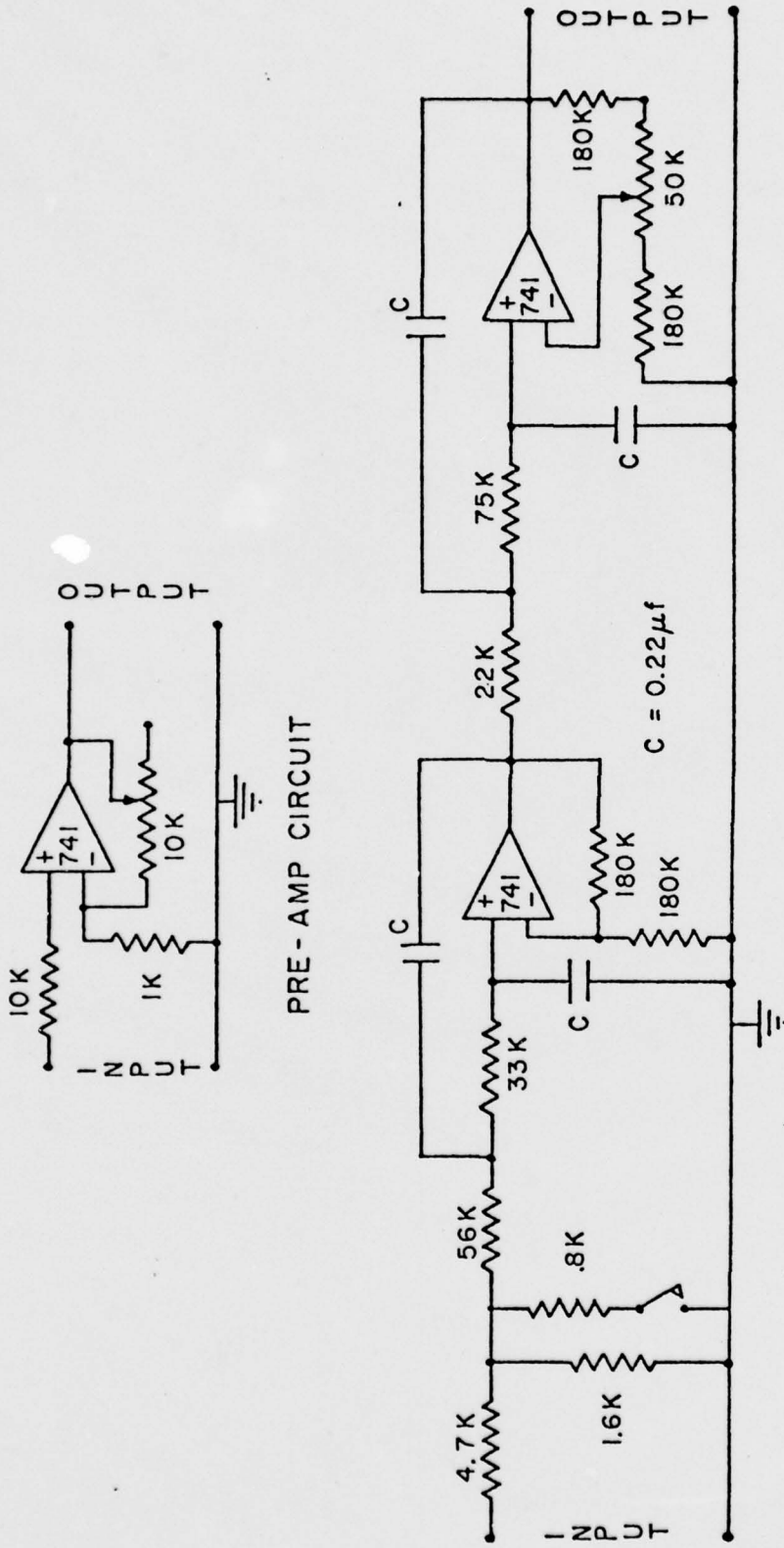


Figure 13. Calibration Curve for Thermistor



LOW-PASS FILTER CIRCUIT

Figure 14. Schematic of Pre-Amp and Filter Circuits



input-impedance and a low output-impedance which acts to isolate the sensors from the recording equipment. The filter circuit is a fourth-order, Butterworth, low-pass filter, with a cutoff frequency of 16.7 Hz. A schematic of the pre-amp and filter circuit is shown in Figure 14. The filter circuit for each channel may be switched in and out as desired. The low-pass filter was not used with the hot-film anemometer.

The Strip Chart Recorder: An eight-channel Visicorder manufactured by Honeywell is connected in parallel to the tape recorder in order to have a visual record of the data.

#### Procedure

Calibration of Instruments: During this experiment, great care was taken to insure the accuracy of the measurements. The position sensor and the temperature probe both exhibit a high degree of stability; therefore, these probes were calibrated only once. Their calibration curves were, however, checked before each test. The hot-film and conductivity probes tend to change calibration over long periods of time (more than one day); therefore, these probes were calibrated immediately before each test.

Before the hot-film probe was mounted in the wave tank it was calibrated in a tow tank. The probe was pulled through still water at a constant speed and the velocity determined by measuring the time required for the probe to traverse a known distance. During this time the anemometer output was fed into an integrator unit manufactured by Disa Company. The average output signal was then plotted against the measured velocity. When enough points were determined a curve was drawn through the points. The salinity of the water in the tow tank was then changed and the process repeated.

The conductivity probe was calibrated in the wave tank immediately before each test as follows: a syphon, which draws water in through a horizontal slot, was mounted at the same level as the conductivity probe. The slots in the syphon and the conductivity probe are the same thickness, therefore, they will both draw fluid by selective withdrawal from the same density level. After the tank was filled the interfacial region between the fresh and salt water was several inches thick (see Figure 16). The conductivity probe and syphon were stepped through the interface. At each level water was drawn off by the syphon. The specific gravity and temperature of this water was measured with a hydrometer and thermometer, and the output voltages from the conductivity probe and thermistor were recorded. The specific gravity of the water drawn off was corrected for temperature changes which may occur during the syphoning process, and the corrected specific gravity was then plotted against the conductivity probe output voltage. This process was repeated at each level until the entire calibration curve was determined. The calibration curve used in this experiment is shown in Figure 11. After the calibration was completed the syphon was removed in order to reduce disturbances to the flow.

Data Acquisition: Two procedures were followed in this experiment to obtain the velocity and density profiles. The first is referred to as a constant speed traverse (CST). In this case the instrument package was moved vertically at a constant speed from the fresh water layer through the interface into the salt water layer. The length of time required to make a traverse in this manner was about 30 sec. This is much shorter than the time scales associated with changes in the velocity and density profiles; therefore, profiles obtained in this way may be thought of as quasi-instantaneous. The second procedure which was followed is referred

to as a stepped traverse (ST). In this case the instrument package was lowered through the interface in steps, and the traverse remained at each level for up to 30 sec. This procedure was designed to determine both the mean velocity profile and the rms value of the velocity fluctuations at different levels through the transition region.

Before the shear flow was started a CST was taken. This was done in order to determine the initial density profile, and to determine the effect of the vertical velocity component on the anemometer reading.

After the flow was started a CST was taken about every ten minutes. Due to the length of time required an ST was taken only once or twice for each flow speed.

Data Reduction: After the tests were completed the data were taken from the magnetic tape and reduced as follows. For each traverse (sometimes referred to as a run) the conductivity, thermistor, and anemometer output voltages were plotted vs. position using the X-Y plotter. The specific gravity at each level was obtained from the conductivity voltage by using Figure 11. If the thermistor indicated a significant temperature change, the specific gravity was corrected for these changes. The velocity at each level was obtained from the anemometer reading and the calibration curve shown in Figure 12. Since the density at each level was known, a linear interpolation between the two curves in Figure 12 was used to correct the anemometer reading for density variations. This reduction procedure was repeated until the velocity and density profiles were complete. These profiles were then used as input to a simple computer program designed to calculate the Richardson number profile. The program uses a weighted average of the forward and backward finite difference calculation to determine the derivatives of the velocity and density at each point.

## CHAPTER V RESULTS AND CONCLUSIONS

Prior to examining the results of this experiment some processes which take place in the tank during the experiment will be discussed. After the shear pump is started the flow initially passes through a transient period before reaching a steady state condition. During the transient period the interface between the fresh and salt water sets-up toward the downstream end of the tank and sharpens rapidly. Following this, disturbances begin to form on the interface.

The generation of the set-up results in a seiching-type motion of the interface which can be observed for several minutes. The calculated period of oscillation, for the stratification used in this experiment, is 55 seconds; this compares well with the observed period.

The rapid sharpening of the interface, which takes place during the first 15 to 20 minutes, starts at the upstream end and moves to the downstream end of the tank. It is not possible to determine from the data taken in this experiment if this process is a natural consequence of the shear flow or if it results from the design of the tank.

Immediately after the interface has become sharp small disturbances begin to form. The upper photograph in Figure 15 is of the disturbances which form at small flow rates (less than 1 in/sec) and the lower photograph shows the disturbance at larger flow rates.

A plot of the interface position vs. time is shown in Figure 16. The data scatter for the first 90 minute period is large. This scatter,

however, may be the result of seiching which has not completely died out. Based on this data, the transient period is estimated to last 90 minutes and the interface erosion rate for the steady state condition is  $3.8 \times 10^{-3}$  in/min. The erosion rates for larger flow rates could not be determined due to an insufficient number of data points. It is unknown if the transients, which result from increasing the flow rate, had died to a tolerable level.

The velocity, density and Richardson number profiles for Runs 1,5, 12,13,15,16 are shown in Figures 17 through 27. It should be noted that Run #5 was made only 30 minutes after the pump was started; therefore, the profiles for this run may have some distortion due to interfacial motion. An important result obtained from the density profiles is that the point of maximum density gradient always falls at  $\xi=0$ . This implies that the inflection point in the density profile always falls at the point where the density is equal to the average density of the upper and lower layer. After the interface has become sharp and the flow has reached equilibrium the maximum density gradient remains constant. For this experiment the maximum gradient was maintained at a value of 0.113 ( $\Delta S.G./in$ ). This value may vary with the flow rate and the degree of stratification.

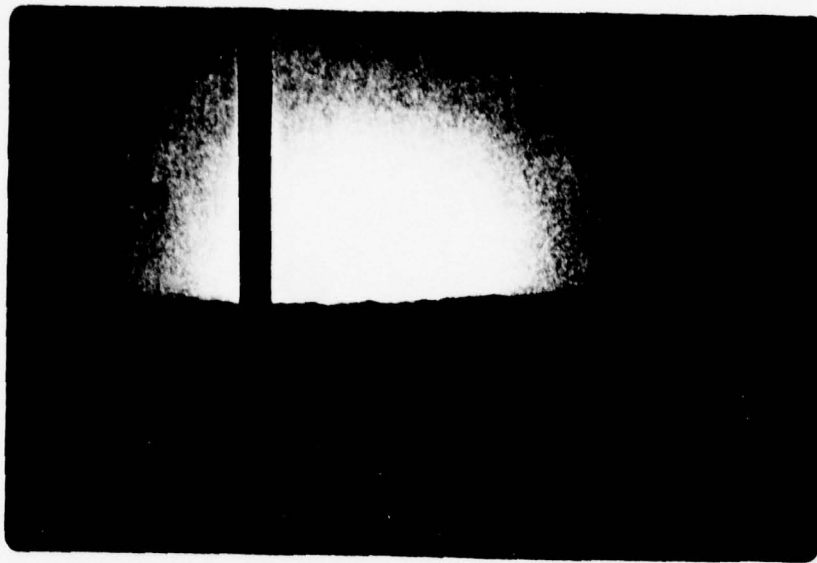
The Richardson number profiles obtained are found to have certain characteristics in common. First, if a Richardson number between 1/4 and 1 is chosen as a criterion for stability, the flow is characterized by an unstable upper and a stable lower region. The point of maximum density gradient ( $\xi=0$ ) is always located a small distance below the boundary separating the two regions. Secondly, the Richardson number profiles all exhibit a shape similar to the profiles found in regions II and III

of Hazel's model. A small distance above  $\xi=0$  the Richardson number profiles have either a local or an absolute maximum. Above this point the Richardson number drops rapidly to zero and below this point the profile passes through a local minimum.

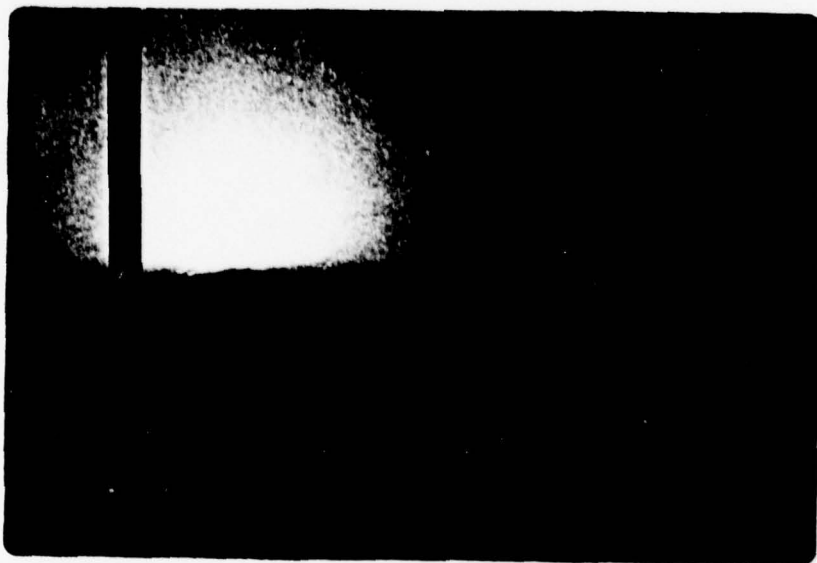
The results of this experiment indicate (for shear flows which are generated in this manner) that the critical point in the Richardson number profile ( $R_i < 1/4$ ) is always found a small but finite distance above the point of maximum density gradient. For this reason instabilities must be initiated at a point above the interface and as these disturbances propagate downward they are quickly dampened by the large stratification. It appears that some of the energy of these disturbances is transformed into small scale wave-type motions at the interface (see Figure 15). As these waves grow and break, part of their energy is transformed to potential energy by raising the center of gravity of the water column.

The results of this investigation have provided the following new information:

- 1). An actual simultaneous measure of the velocity and density profiles in a two layer stratified shear flow;
- 2). A measurement of the Richardson number profile for this flow, which shows that the critical point in the Richardson number profile always falls above the point of maximum density gradient.
- 3). The inflection point of the density profile, which is also the point of maximum density gradient, is found at  $\xi=0$  and,
- 4). The interfacial erosion (or dispersion) rate under known distributions of velocity, density and Richardson number.



Low Flow Rates ( $< 1$  in/sec)



Higher Flow Rates

Figure 15. Photographs of Interfacial Disturbance

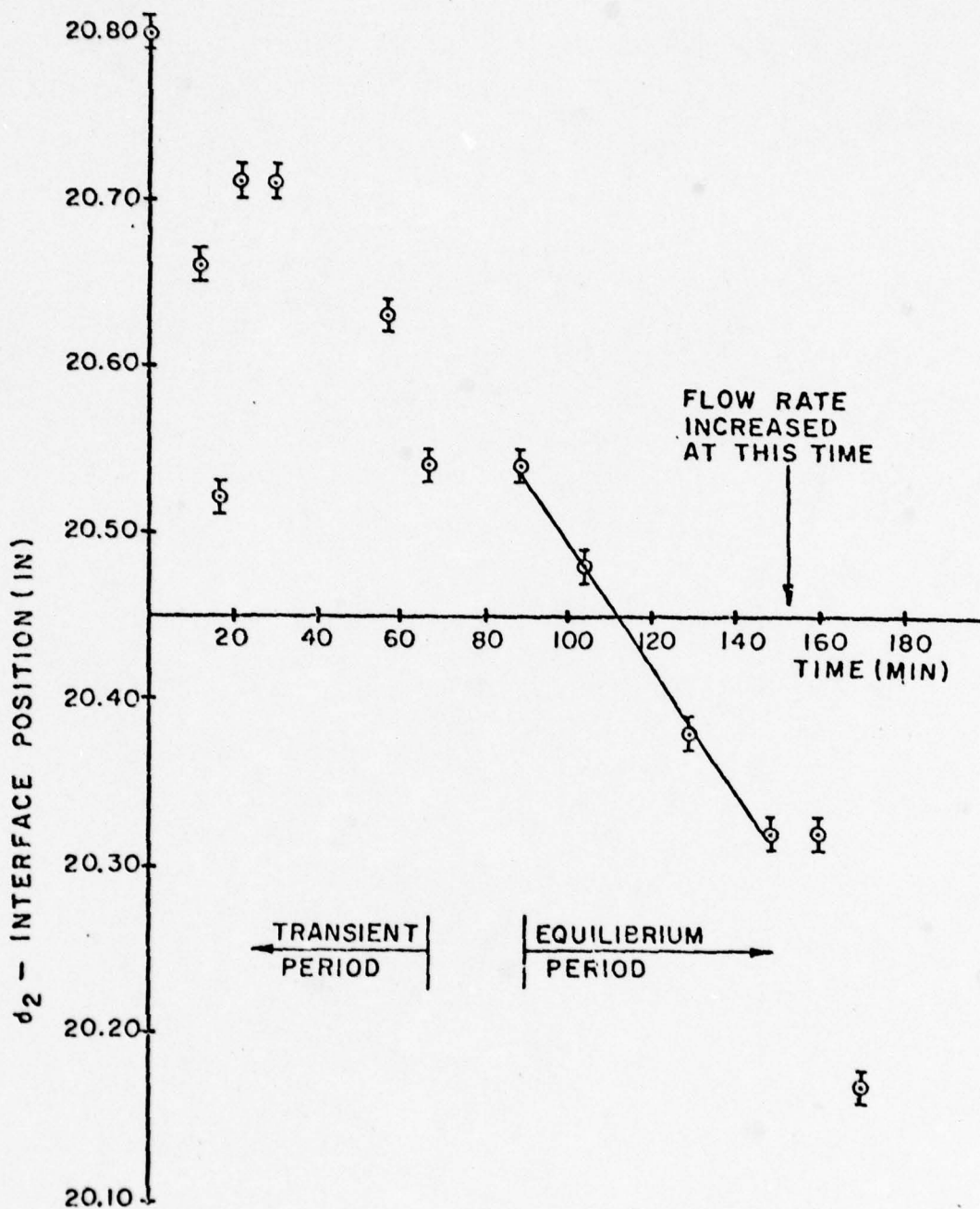


Figure 16. Plot of Interface Position vs. Time



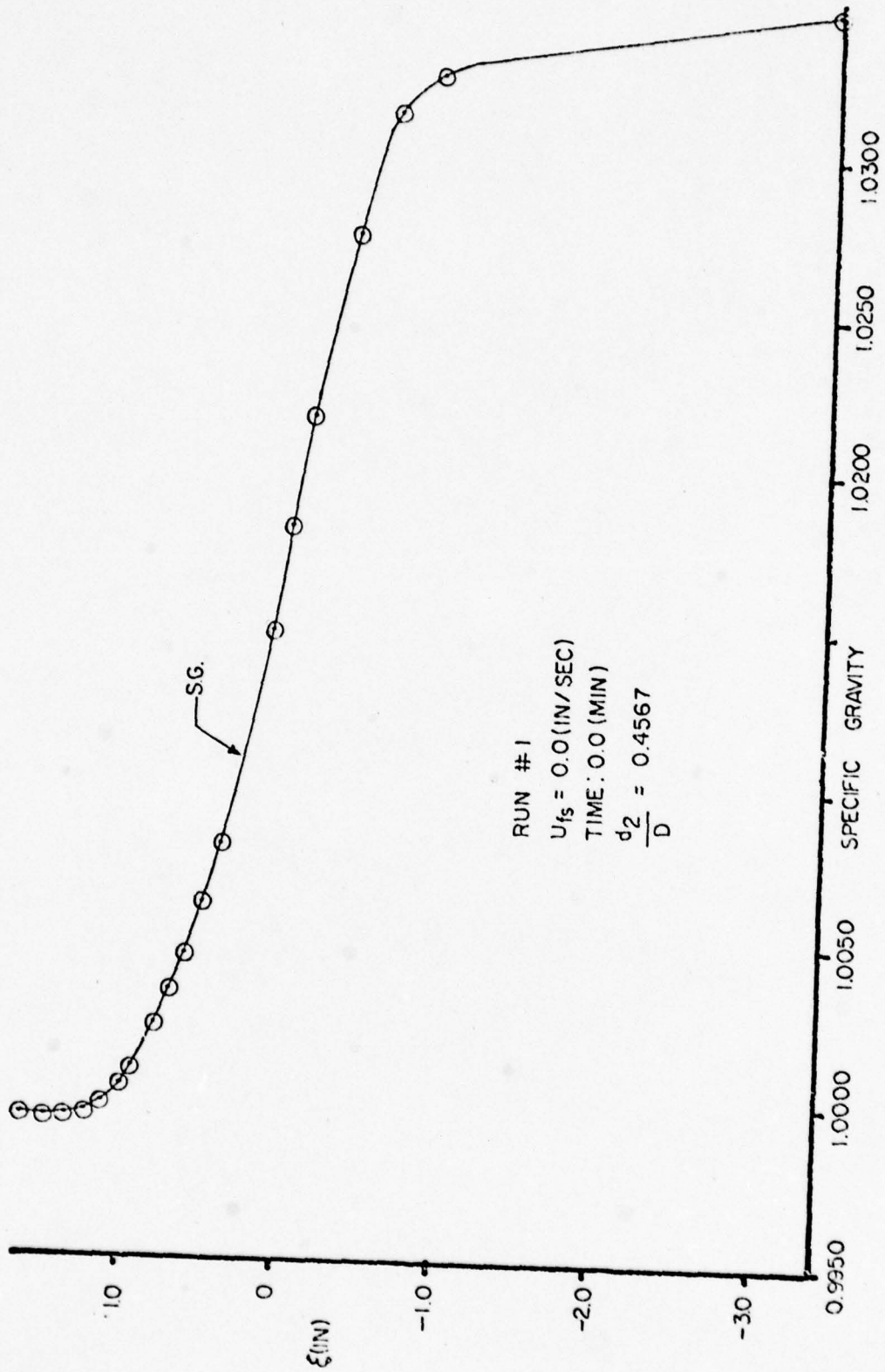


Figure 17. Initial Density Profile Before Shear Flow is Started

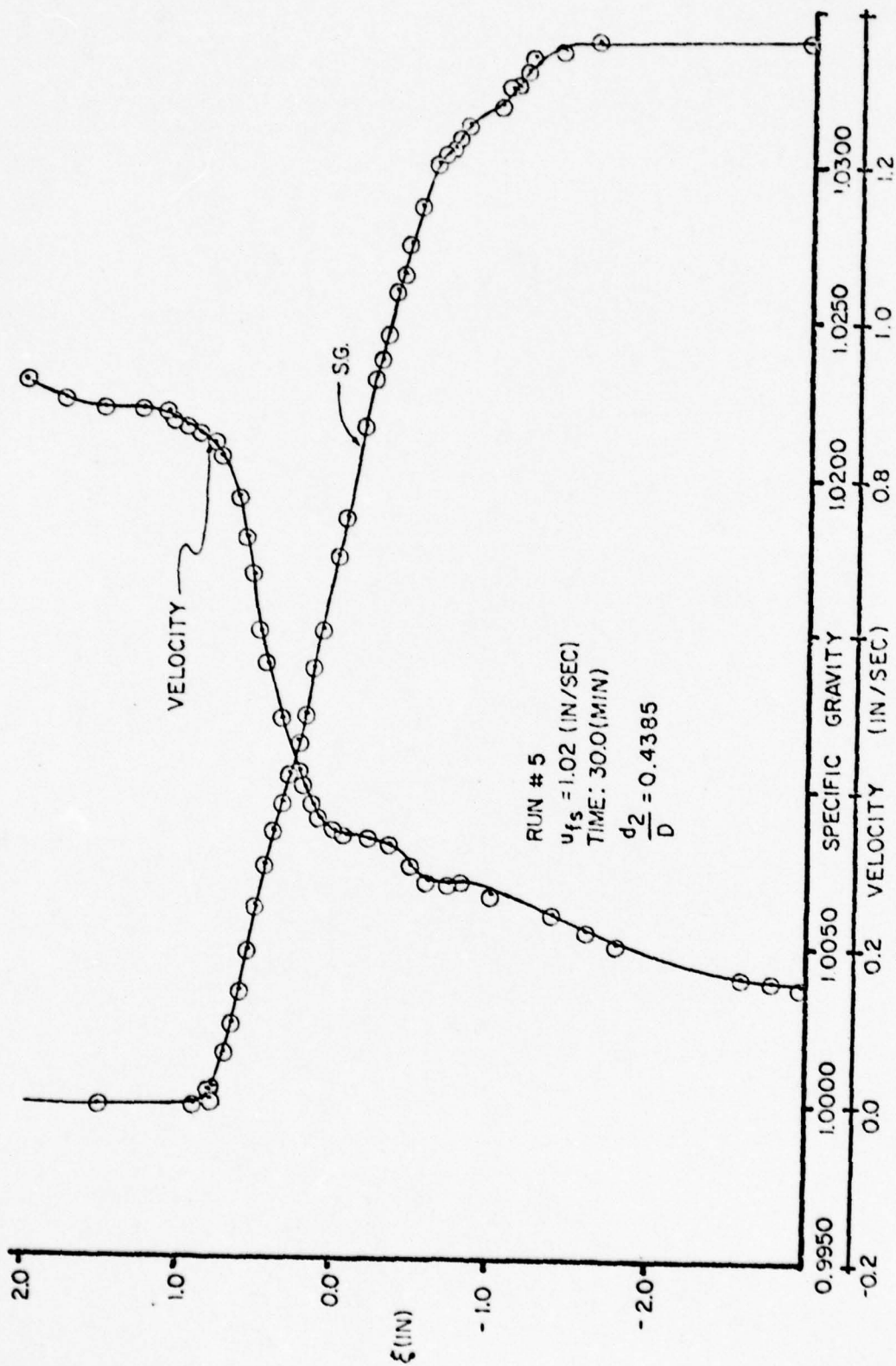


Figure 18. Velocity and Density Profiles, Run #5

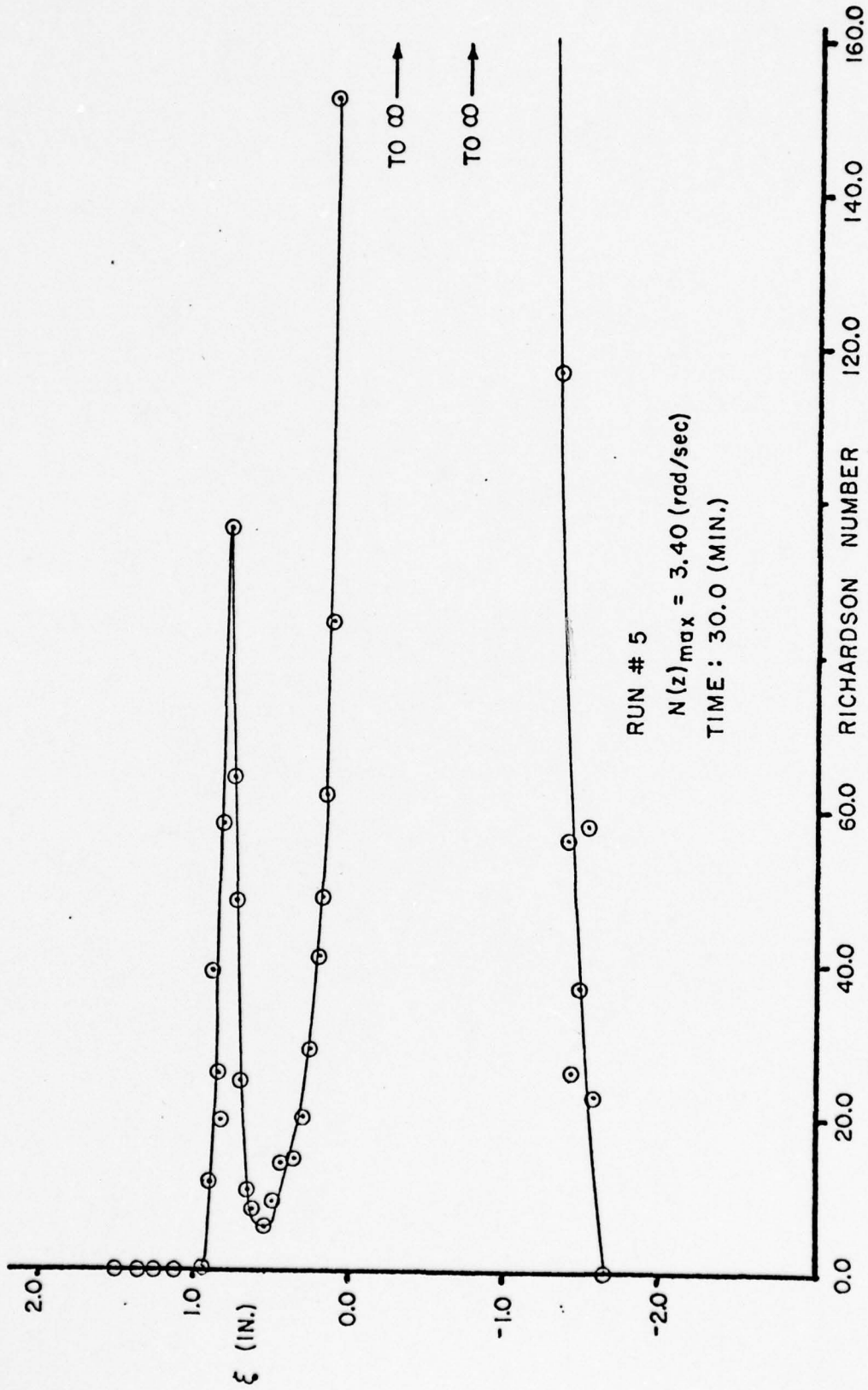


Figure 19. Richardson Number Profile, Run #5

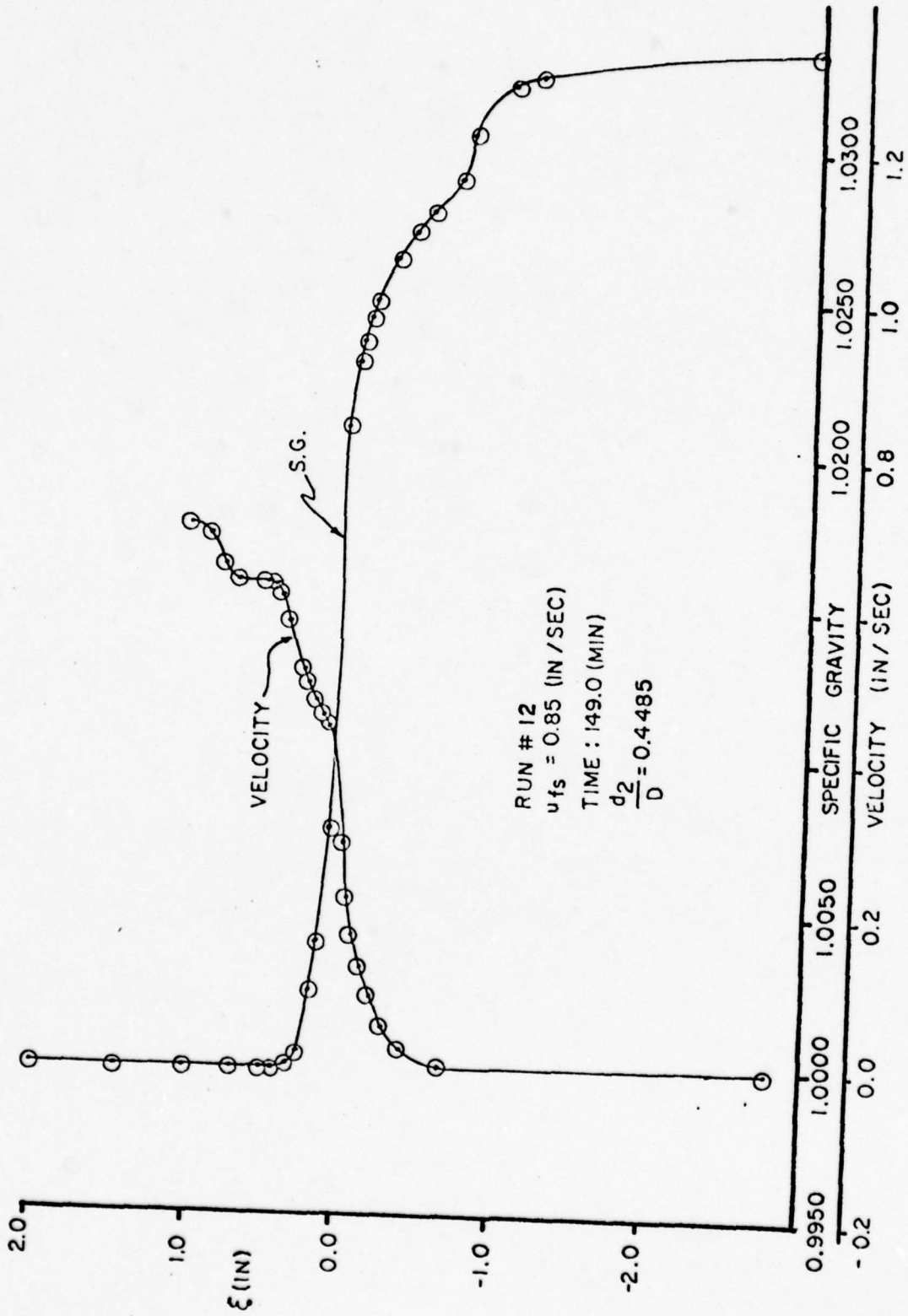


Figure 20. Velocity and Density Profiles, Run #12

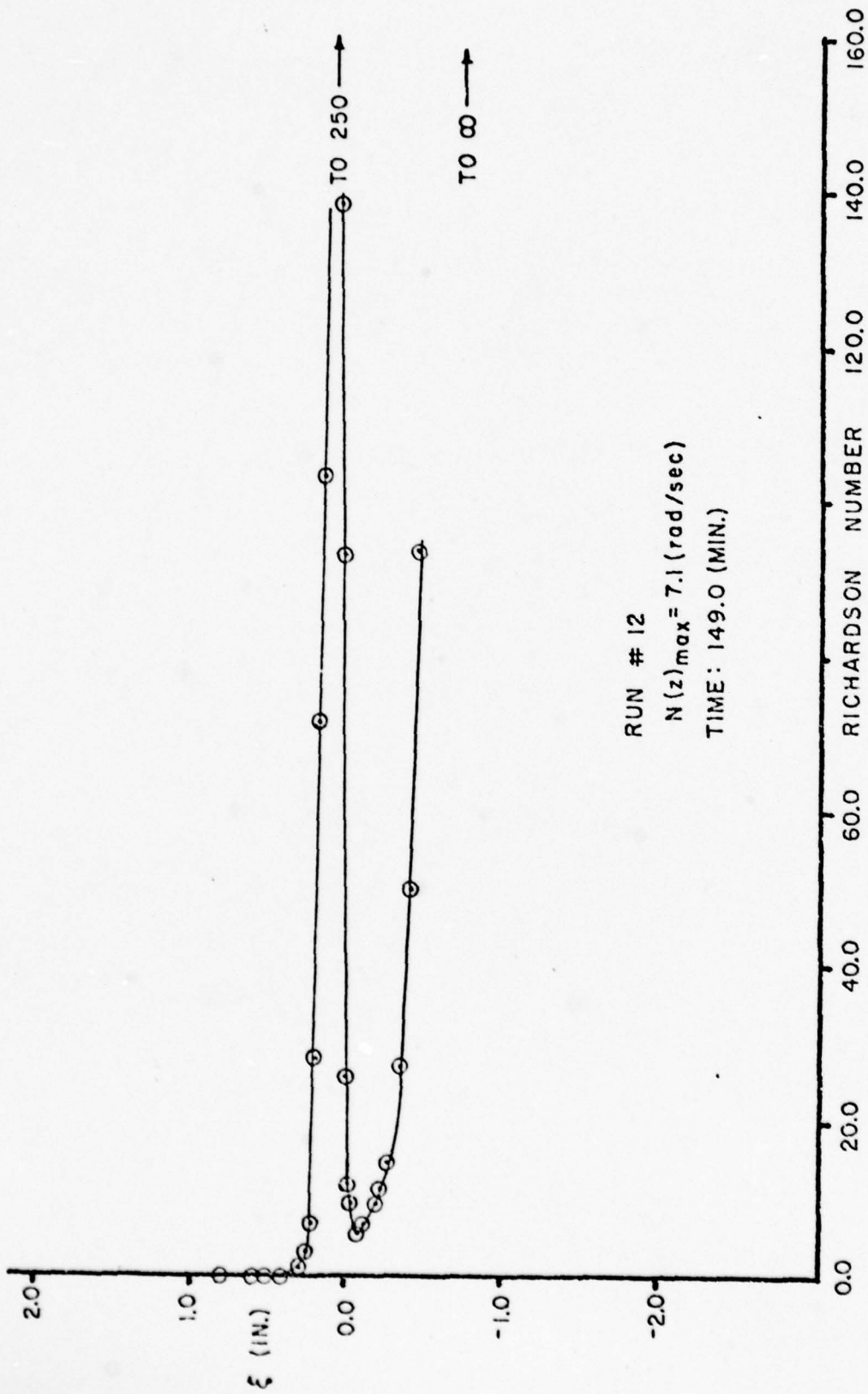


Figure 21. Richardson Number Profiles, Run #12

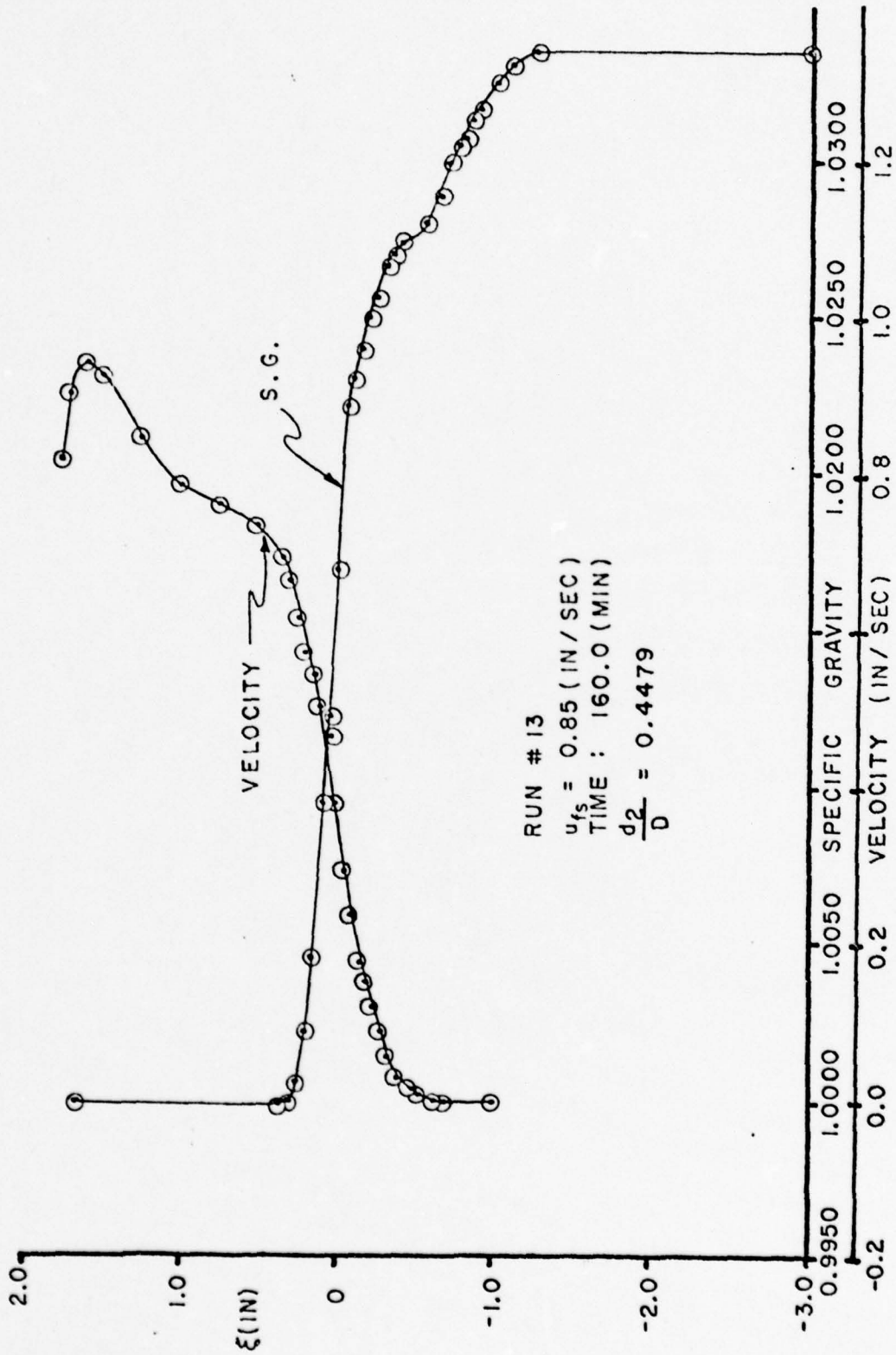


Figure 22. Velocity and Density Profiles, Run #13

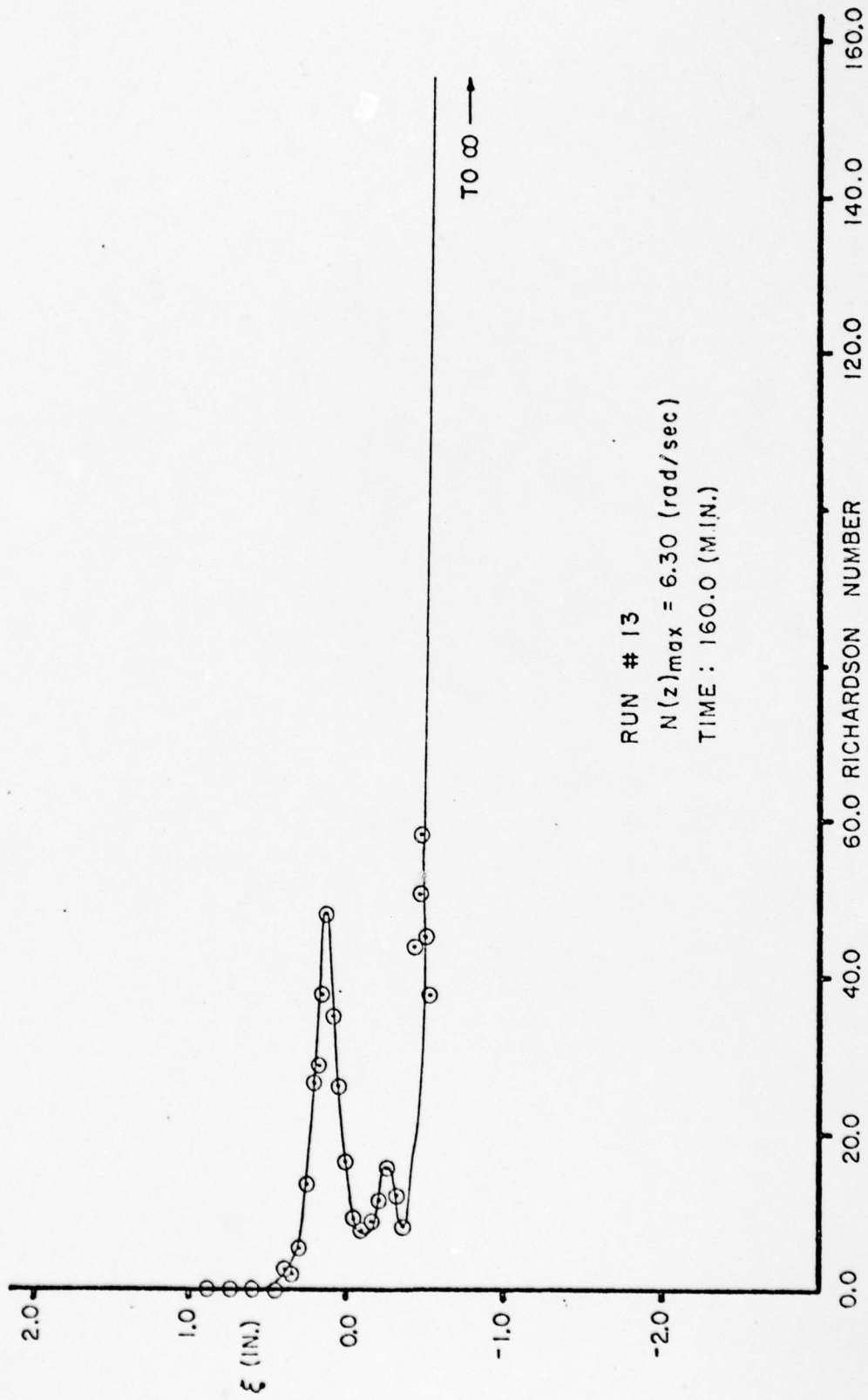


Figure 23. Richardson Number Profile, Run #13

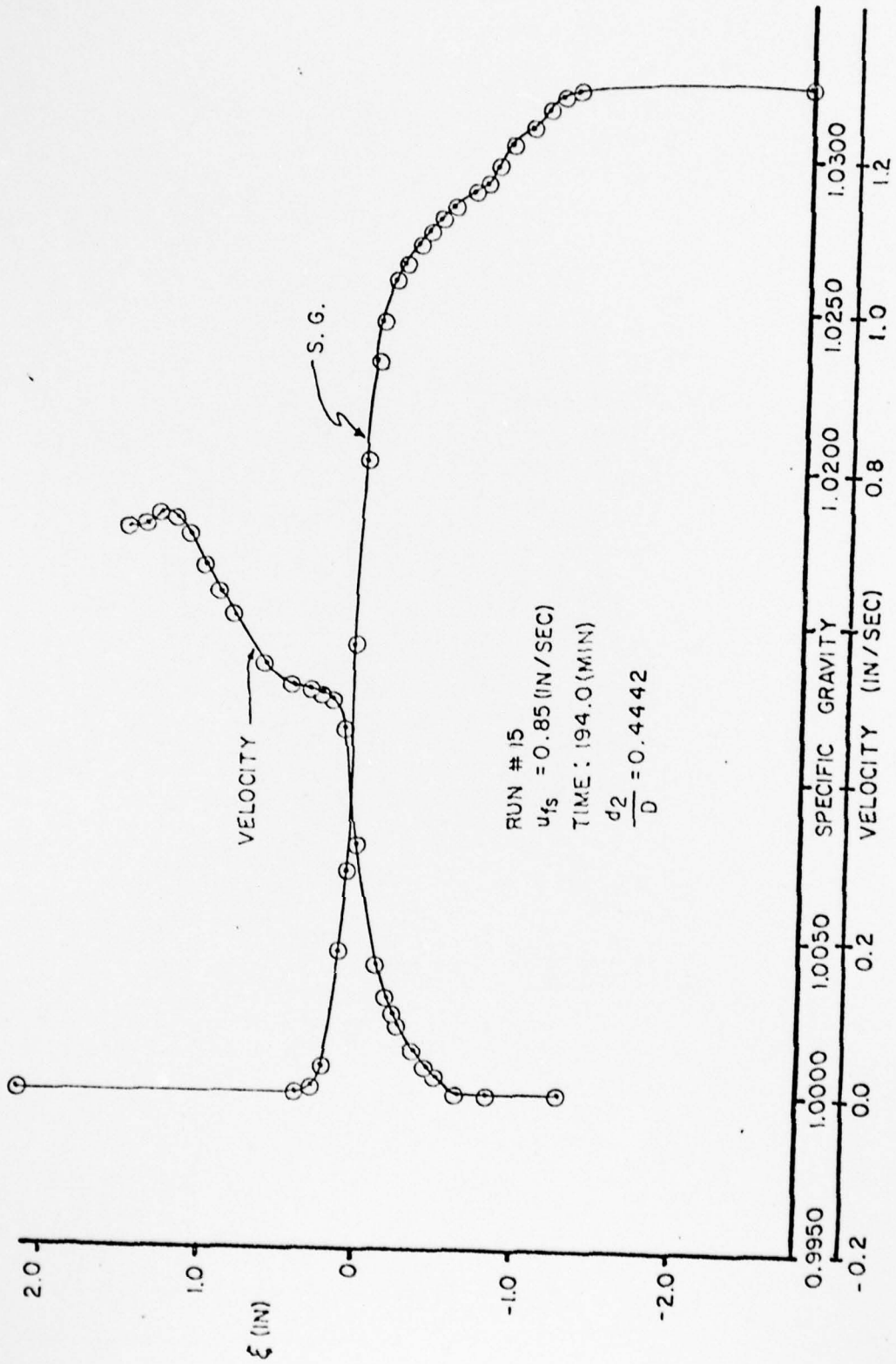


Figure 24. Velocity and Density Profiles, Run #15



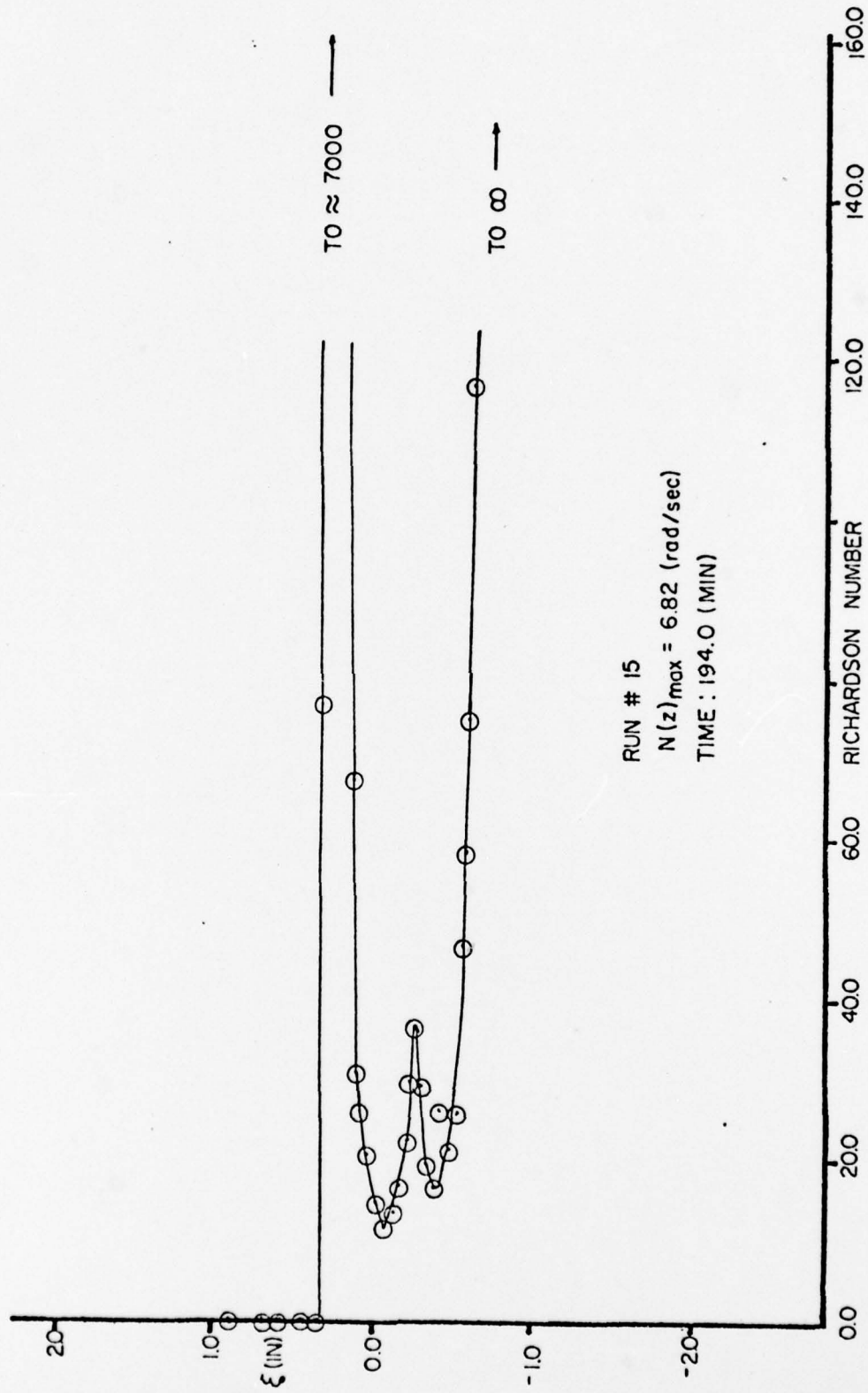


Figure 25. Richardson Number Profile, Run #15

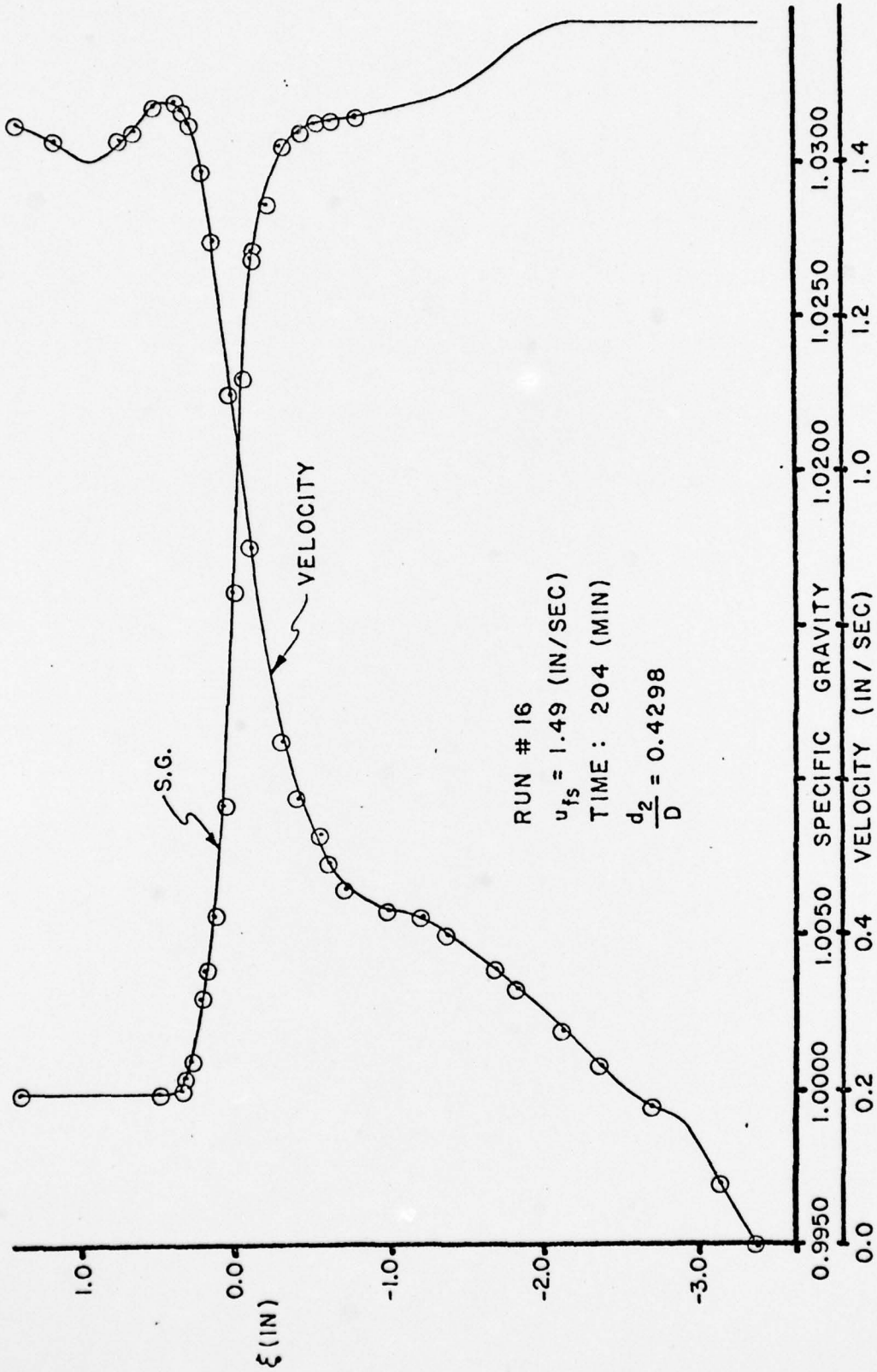


Figure 26. Velocity and Density Profiles, Run #16

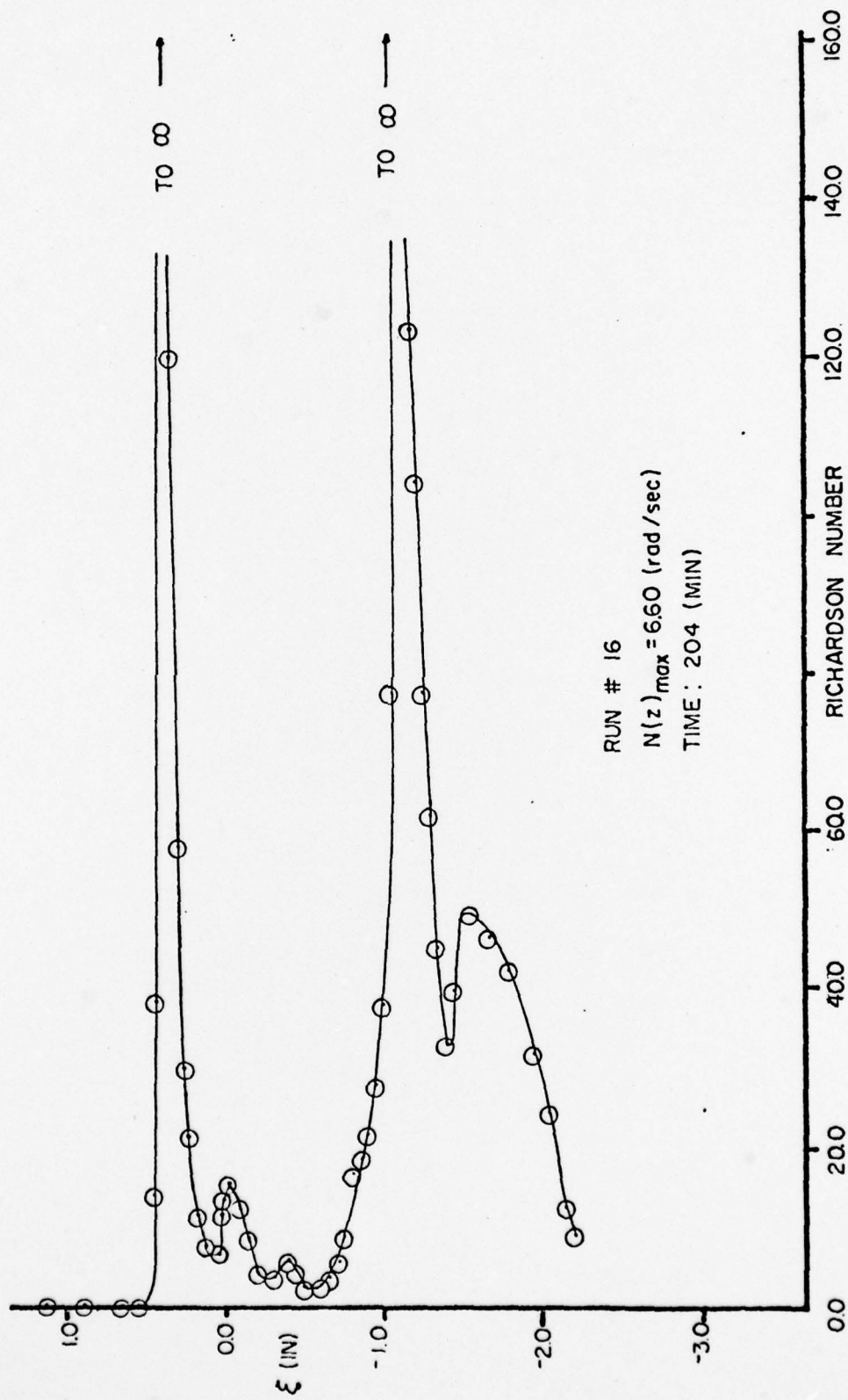


Figure 27. Richardson Number Profile, Run #16

## CHAPTER VI FUTURE STUDIES

The finite amount of time allotted to any experiment always results in more questions than answers. Some of the questions which surfaced during this experiment, but remain unanswered, are discussed below.

As an extension of this work, it would be desirable to obtain more data for different flow rates and different degrees of stratification at several locations down the tank. It may then be possible to determine if these changes affect the characteristic shape of the Richardson number profiles. The relationship between the flow rate, the stratification and the maximum density gradient could also be determined.

It was not possible, due to the small velocities and the type of hot-film probe used in this experiment (wedge-type), to measure the velocity fluctuations. A knowledge of these fluctuations would help in understanding the mixing process which takes place at the interface. This information could be obtained in future experiments by using a cylindrical hot-film probe.

The rapid sharpening of the interface which occurs during the first 15 to 20 minutes is not yet understood. In the future it may be helpful to take more data during this period.

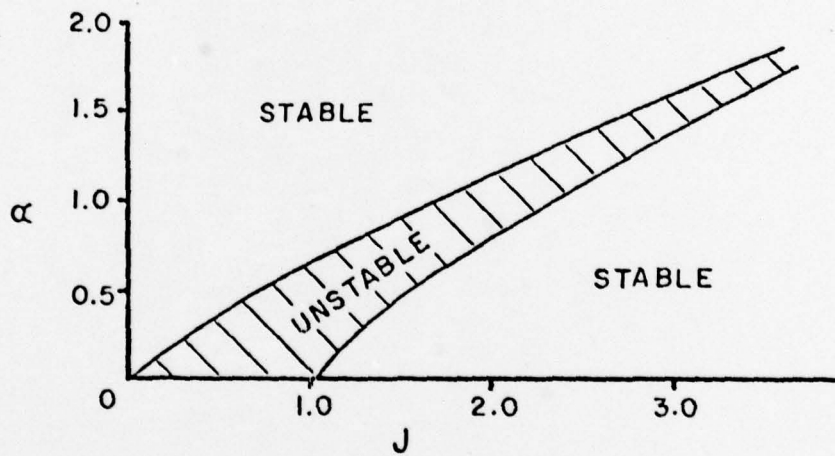
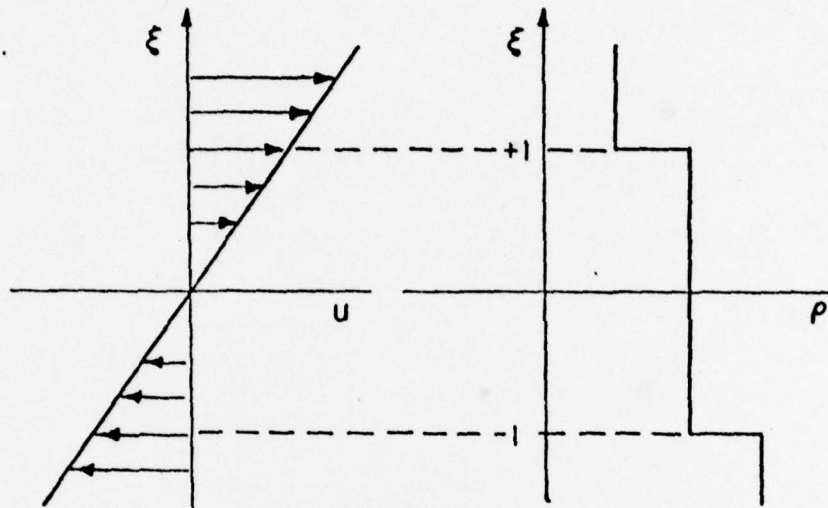
APPENDIX  
SOME ANALYTIC SOLUTIONS TAKEN FROM THE LITERATURE

The analytic solutions presented on the following pages are only a few of the solutions obtained by various investigators. They are presented here to stress the points made in Chapter II; namely, that the solution to the stability problem is highly dependent on the shape of the velocity and density profiles and that the solutions which have been obtained are not always indicative of reality. Note that the Taylor model is stable over all  $\alpha$  for  $J=0$ ; while the Taylor and Goldstein model is unstable over a finite range of  $\alpha$  for  $J=0$ .

TAYLOR

$$u = \xi$$

$$\beta = \frac{\rho'}{\rho} = \delta(\xi+1) + \delta(\xi-1)$$



FLOW IS UNSTABLE FOR:

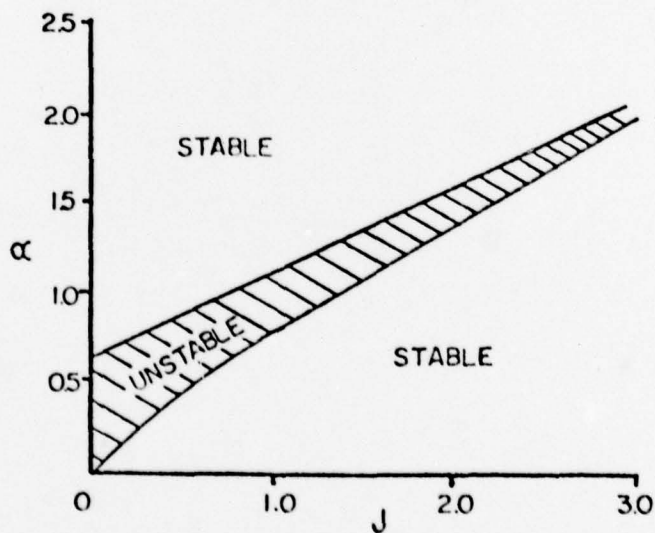
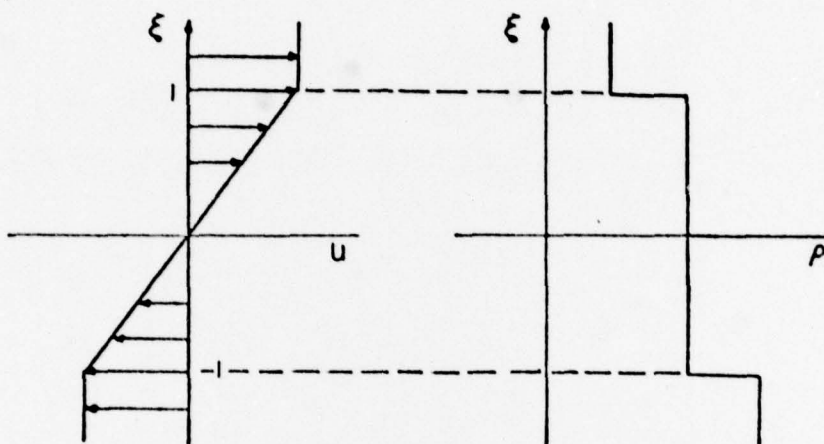
$$\frac{2\alpha}{1+e^{-2\alpha}} < J < \frac{2\alpha}{1-e^{-2\alpha}}$$

Figure 28. Taylor Stability Model

TAYLOR AND GOLDSTEIN

$$u = \begin{cases} \text{Sgn } \xi & (|\xi| > 1) \\ \xi & (|\xi| \leq 1) \end{cases}$$

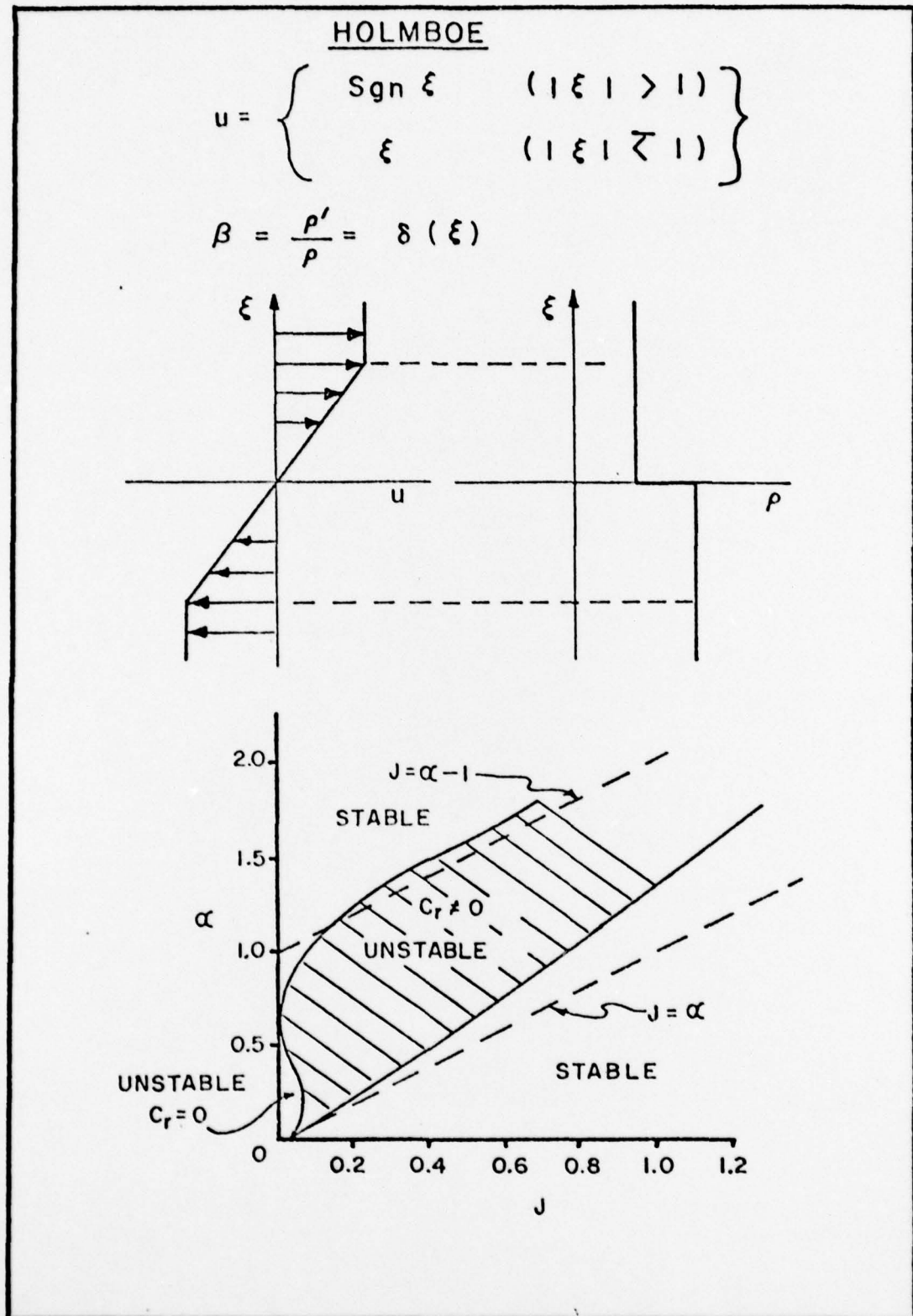
$$\beta = \frac{\rho'}{\rho} = \delta(\xi+1) + \delta(\xi-1)$$



FLOW IS UNSTABLE FOR:

$$\frac{2\alpha}{1+e^{-2\alpha}} - 1 < J < \frac{2\alpha}{1-e^{-2\alpha}} - 1$$

Figure 29. Taylor and Goldstein Stability Model





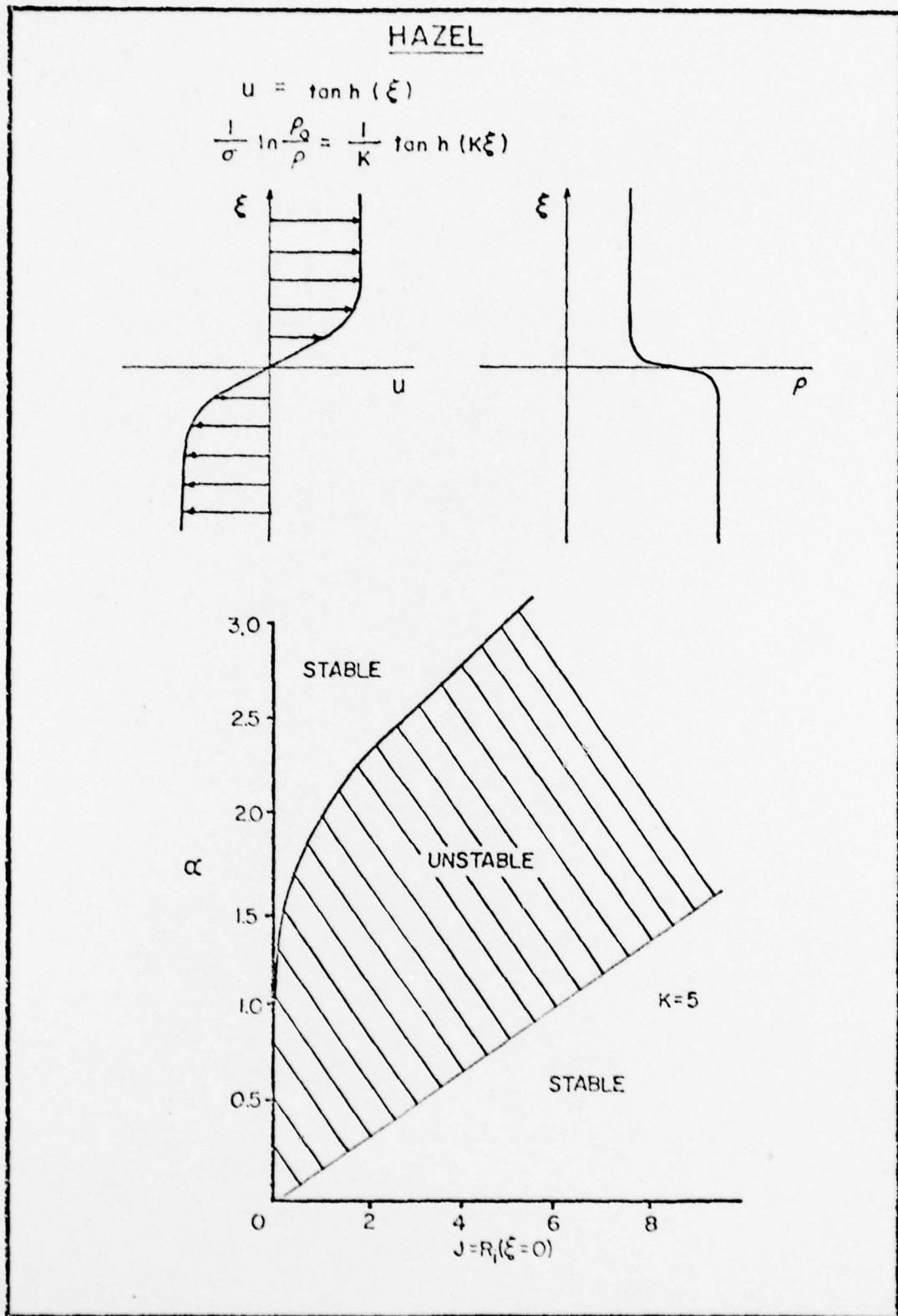


Figure 31. Hazel's Numerical Model

## BIBLIOGRAPHY

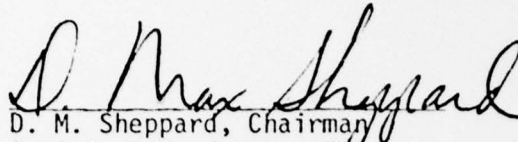
- Broward, F.K. and Winant, C.D., (1972), "Laboratory Observations of Shear-Layer Instability in a Stratified Fluid.", Boundary-Layer Meteorology 5, 67-77.
- Drazin, P.G. and Howard, L.N., (1966), "Hydrodynamic Stability of Parallel Flow of Inviscid Fluid," Advanc. Appl. Mech. 9, 1-89.
- Fleagle, R.G., (1969), "The Significance of Clear Air Turbulence in Large Scale Meteorology," Clear Air Turbulence and Its Detection, Plenum Press, N.Y., 1-3.
- Goldstein, S. (1931), "On the Stability of Superposed Streams of Fluids of Different Densities.", Proc. Roy. Soc., A 132, 525-48.
- Hazel, P. (1972), "Numerical Studies of the Stability of Inviscid Stratified Flows," J. Res. Nat. Bur. Stand., 43, 487-500.
- Howard, L.N., (1961), "Note on a Paper of John W. Miles," J. Fluid Mech., 10, 509-12.
- Howard, L.N. and Moslowe, S.A., (1972), "Stability of Stratified Shear Flows," Boundary-Layer Meteorology 4, 511-523.
- Keulegan, G.H., (1949), "Interfacial Instability and Mixing in Stratified Flows," J. Res. Nat. Bur. Stand., 43, 487-500.
- Long, R.R., (1972), "Some Properties of Horizontally Homogeneous, Statistically Steady Turbulence in a Stratified Fluid.", Boundary-Layer Meteorology 5, (1973), 139-157.
- Miles, J.W., (1961), "On the Stability of Heterogeneous Shear Flows.", J. Fluid Mech. 10, 496-508.
- Scotti, R.S. and Corcos, G.M., (1969), "Measurements on the Growth of Small Disturbances in a Stratified Shear Layer," Radio Science 4, 1309-13.
- Taylor, G.I., (1931a), "Effect of Variation of Density on the Stability of Superposed Streams of Fluid.", Proc. Roy. Soc., A132, 499-523.
- Thorpe, S.A., (1969c), "Experiments on the Stability of Stratified Shear Flows," Radio Science, 4, 1327-31.

- Wang, Y.H., (1972), "An Experimental Study of a Discontinuously Stratified Shear Layer", Ph.D. Thesis, University of Southern California.
- Woods, J.D., (1969), "On Richardson's Number as a Criterion for Laminar-Turbulent-Laminar Transition in the Atmosphere and Ocean," Radio Science, 4, 1289-98.

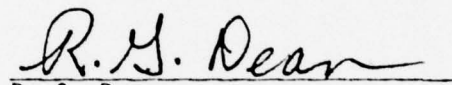
#### BIOGRAPHICAL SKETCH

Gregory M. Powell was born November 1, 1949 in Milwaukee, Wisconsin. He spent his youth in Miami, Florida, where his parents moved while he was still an infant. In June, 1968, he was graduated from North Miami High School in North Miami, Florida. He received a Bachelor of Science degree in Aerospace Engineering from the University of Florida in December, 1972 and immediately entered graduate school in the Department of Coastal and Oceanographic Engineering at the University of Florida. He has worked as a graduate assistant while earning a Master of Engineering degree. He is married to Carol Brady.

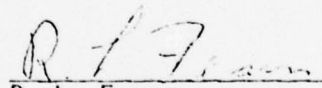
I certify that I have read this study and that in my opinion it conforms to acceptable standards of scholarly presentation and is fully adequate, in scope and quality, as a thesis for the degree of Master of Engineering.

  
D. M. Sheppard, Chairman  
Assistant Professor of  
Engineering Sciences

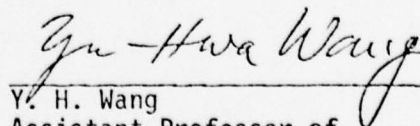
I certify that I have read this study and that in my opinion it conforms to acceptable standards of scholarly presentation and is fully adequate, in scope and quality, as a thesis for the degree of Master of Engineering.

  
R. G. Dean  
Professor of Engineering Sciences

I certify that I have read this study and that in my opinion it conforms to acceptable standards of scholarly presentation and is fully adequate, in scope and quality, as a thesis for the degree of Master of Engineering.

  
R. L. Fearn  
Assistant Professor of  
Engineering Sciences

I certify that I have read this study and that in my opinion it conforms to acceptable standards of scholarly presentation and is fully adequate, in scope and quality, as a thesis for the degree of Master of Engineering.

  
Y. H. Wang  
Assistant Professor of  
Engineering Sciences

This thesis was submitted to the Dean of the College of Engineering and to the Graduate Council, and was accepted as partial fulfillment of the requirements for the degree of Master of Engineering.

March, 1975

\_\_\_\_\_  
Dean, College of Engineering

\_\_\_\_\_  
Dean, Graduate School